


 Cite this: *RSC Adv.*, 2025, 15, 1134

Received 27th November 2024

Accepted 6th January 2025

DOI: 10.1039/d4ra08384a

rsc.li/rsc-advances

Transition metal-catalyzed cross-coupling reactions of *N*-aryl-2-aminopyridines

 Fatemeh Doraghi,^a Lina Rezainia,^b Mohammad Hossein Morshedsolouk,^{ab} Hamed Navid,^b Bagher Larijani^a and Mohammad Mahdavi^{*,a}

Due to the presence of the pyridyl directing group, *N*-aryl-2-aminopyridines can quickly form stable complexes with metals, leading to cyclization and functionalization reactions. A large number of *N*-heterocycles and nitrogen-based molecules can be easily constructed *via* this direct and atom-economical cross-coupling strategy. In this review, we have highlighted the transformations of *N*-aryl-2-aminopyridines in the presence of various transition metal catalysts, such as palladium, rhodium, iridium, ruthenium, cobalt and copper.

1. Introduction

Transition metal-catalyzed directing group-assisted heteroannulations of amines with other coupling partners have emerged as a powerful and efficient tool.^{1–5} *N*-Heterocyclic compounds are the main nuclei in functional materials,^{6,7} pharmaceuticals^{8–11} and natural products.^{12–14} Consequently, various straightforward and affordable routes have been developed for synthesizing bioactive *N*-heterocycles. Among them, nitrogen-directing group-assisted substrates, leading to *ortho*-selective C–H activation are very popular. The nitrogen auxiliary

groups form a variety of stable metal complexes and are then easily removed or undergo further transformations.

N-Aryl-2-aminopyridines, which are readily prepared by the coupling of anilines with 2-bromopyridines,^{15–17} are extensively used as substrates in the context of C–H activation. Owing to the presence of the pyridyl as a directing group, *N*-aryl-2-aminopyridines can easily incorporate into the chelation-assisted C–H bond functionalization. Various transition metals, such as palladium, rhodium, iridium, ruthenium, cobalt and copper can be involved in the formation of five-, six- and seven-membered complex intermediates with the nitrogen-pyridyl group through the coordination and C–H bond activation process. A diverse range of bioactive *N*-heterocycles, including indoles, carbazoles, quinolinones, benzimidazoles, indolinones, imidazopyridines and functionalized *N*-aryl-2-aminopyridines can be obtained *via* annulation or

^aEndocrinology and Metabolism Research Center, Endocrinology and Metabolism Clinical Sciences Institute, Tehran University of Medical Sciences, Tehran, Iran. E-mail: momahdavi@tums.ac.ir

^bSchool of Chemistry, College of Science, University of Tehran, Tehran, Iran


Fatemeh Doraghi

Fatemeh Doraghi received her bachelors and masters degrees in organic chemistry from Shahid Chamran University, Ahvaz in 2008 and 2014, respectively. She received her PhD degree in organic chemistry from University of Tehran, Tehran in 2022. During her PhD research, she focused on the development of new synthetic methodologies via transition metal as well as metal-free oxidative coupling reactions. She is currently

employed as a researcher at the Endocrinology and Metabolism Research Center, Tehran University of Medical Sciences, Tehran, Iran.


Lina Rezainia

Lina Rezainia was born in 2002 in Tehran, Iran. She received her bachelors degree in pure chemistry from the University of Tehran, Iran in 2024, and graduated with honors. Before receiving her degree, she started doing research in organic synthesis, as well as polymer chemistry.



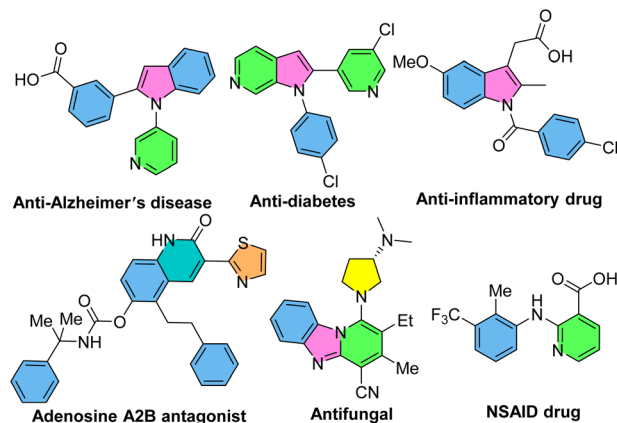
functionalization of *N*-aryl-2-aminopyridines.^{18–23} Some of biologically active compounds containing these valuable cores are depicted in Scheme 1.

Considering the importance of *N*-aryl-2-aminopyridine derivatives, we have highlighted the developments related to these synthons. In this context, we have discussed the annulation and functionalization of *N*-aryl-2-aminopyridine in the presence of transition metal catalysts. We have categorized this review based on the metal type to provide a better insight into the behaviour of each metal catalyst in the presence of *N*-aryl-2-aminopyridines.

2. Transition metal-catalyzed cross-coupling of *N*-aryl-2-aminopyridines

2.1. Pd-catalyzed cross-coupling of *N*-aryl-2-aminopyridines

2.1.1. Annulation. In 2011, Li's research group performed a study on the Pd(II)-catalyzed synthesis of *N*-(2-pyridyl)indole



Scheme 1 Some pharmaceutically important nitrogen-containing compounds.



Mohammad Hossein Morshedsolouk

Mohammad Hossein Morshedsolouk is currently a second-year polymer chemistry student at the University of Tehran. He obtained his bachelors degree in practical chemistry from Shahid Beheshti University. Presently, he is affiliated with the Research Center for Membrane Technology at the University of Tehran. Last year, he worked at the Endocrinology and Metabolism Clinical Sciences Institute at Tehran University of Medical Sciences, where his research focused on the synthesis of various organic compounds. Currently, he is engaged in the study of polymeric membranes and exploring approaches to enhance their performance.



Bagher Larijani

Bagher Larijani was born in 1961 in Iran. He obtained his MD from Tehran University, in 1986. His current research interests focus on diabetes.



Hamed Navid

compounds.

Hamed Navid was born in 1991 in West Azerbaijan Province, Iran. He received his masters degree in organic chemistry from University of Tehran, Tehran in 2020. His thesis was on the assembly of indole cores through a palladium-catalyzed metathesis of Ar-X σ -bonds. He is currently employed as a manager by Azin Polymer Asia Company, in Tehran, Iran. At the moment he is focused on the development of new polymer

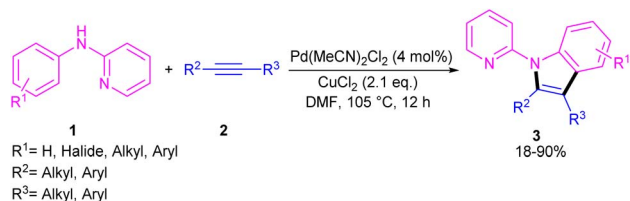


Mohammad Mahdavi

Mohammad Mahdavi was born in 1981 in Tehran, Iran. He received his M.Sc. from the University of Tehran in 2008 and his PhD degree in medicinal chemistry from the Tehran University of Medical Science, Tehran, Iran, in 2016. Since August 2017, he has been with the Endocrinology and Metabolism Research Center, Endocrinology and Metabolism Clinical Sciences Institute, Tehran University of Medical Sciences, Tehran, Iran where he is an Assistant Professor. His current research interests focus on the synthesis of heterocyclic compounds with biological activities.

Mohammad Mahdavi was born in 1981 in Tehran, Iran. He received his M.Sc. from the University of Tehran in 2008 and his PhD degree in medicinal chemistry from the Tehran University of Medical Science, Tehran, Iran, in 2016. Since August 2017, he has been with the Endocrinology and Metabolism Research Center, Endocrinology and Metabolism Clinical Sciences Institute, Tehran University of Medical Sciences, Tehran, Iran where he is an Assistant Professor. His current research interests focus on the synthesis of heterocyclic compounds with biological activities.

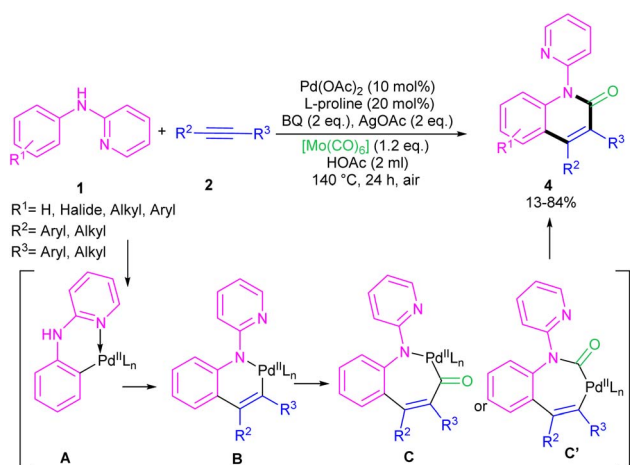




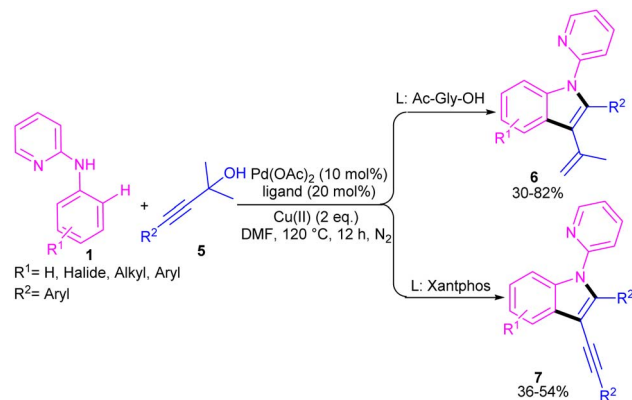
Scheme 2 Pd(II)-catalyzed annulation of *N*-aryl-2-aminopyridine and alkynes.

frameworks **3** through the annulation of *N*-aryl-2-aminopyridines **1** with internal alkynes **2** (Scheme 2).²⁴ In this synthetic method, 4 mol% of Pd(MeCN)₂Cl₂ as a catalyst, 1.2 equiv. of CuCl₂ and O₂ atmosphere as the oxidants were used in DMF solvent. It should be noted that this palladium(II) system did not prove effective for the reaction of *N*-aryl-2-aminopyridines with acrylates towards *N*-(2-pyridyl)quinolones, as these products were achieved in the presence of a Rh(III) catalyst. However, in Wu's laboratory, *N*-(2-pyridyl)quinolones were well synthesized from the annulation of *N*-aryl-2-aminopyridines **1**, internal alkynes **2** and Mo(CO)₆ as a CO source through a (3 + 2 + 1)-cycloaddition process (Scheme 3).²⁵ The currently accepted mechanism involved the initial C-H activation of substrate **1** with Pd(II), followed by the insertion of an alkyne to produce intermediate **B**. Subsequent coordination and insertion of CO to **B** led to intermediate **C** or **C'**, which upon reductive elimination gave product **4**. The generated Pd(0) was re-oxidized by BQ and AgOAc to the active Pd(II) species.

In 2021, Zhou's group reported the assembly of *N*-pyridoindoles **6**, **7** by using *N*-aryl-2-aminopyridines **1** and propargylic alcohols **5** (Scheme 4).²⁶ The catalytic system involved Pd(OAc)₂ as a catalyst, Cu(OAc)₂ or CuSO₄ as an oxidant, Ac-Gly-OH or xantphos as a ligand. Other metal catalysts, such as Co(OAc)₂·4H₂O, Ni(OAc)₂·4H₂O, [RuCl₂(*p*-cymene)]₂ and [Cp*RhCl₂]₂ were not workable as much as Pd(OAc)₂. The indole products were isolated in moderate to high yields (30–82%). Another Pd-catalyzed cyclization reaction between *N*-aryl-2-



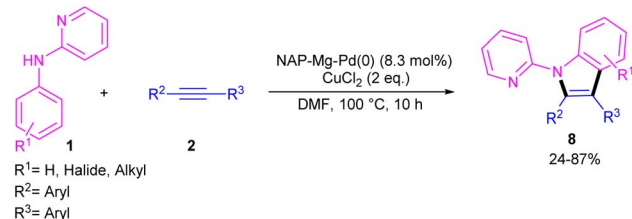
Scheme 3 Pd(II)-catalyzed annulation of *N*-aryl-2-aminopyridine, alkynes and Mo(CO)₆.



Scheme 4 Pd(II)-catalyzed annulation of *N*-aryl-2-aminopyridines with propargylic alcohols.

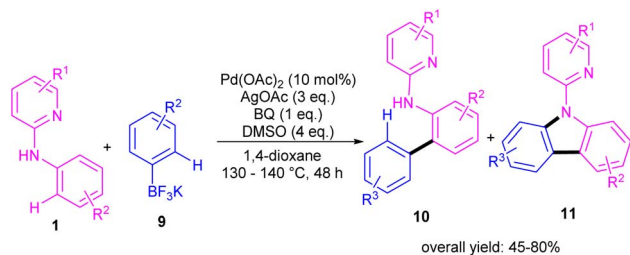
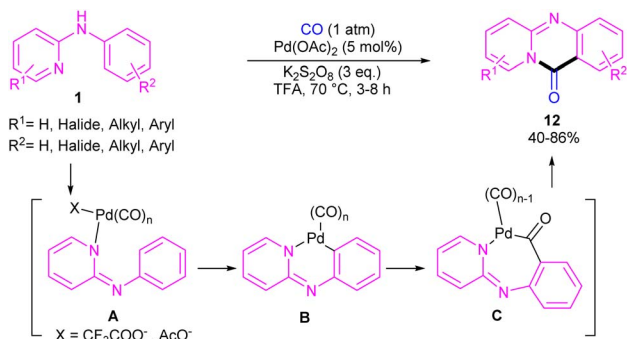
aminopyridines and alkynes access to indoles was reported by Hu and co-workers.²⁷ PdCl₂ as a catalyst, Cu(TFA)₂·xH₂O as an oxidant, and DTBP as a co-oxidant efficiently catalyze this (3 + 2)-cycloaddition process. Nano magnesium oxide can stabilize Pd(0) leading to a heterogeneous nanocatalyst for the C-H activation/annulation of *N*-aryl-2-aminopyridines **1** with alkynes **2** (Scheme 5).²⁸ As an oxidant, CuCl₂ was more practical than the Ag salts, TBHP or O₂ atm. Many *N*-(2-pyridyl)indole products **8** were isolated in good yields by simple operation. Besides, *N*-aryl-2-aminoquinoline and *N*-aryl-2-aminopyrimidine were also yielded the products in 24% and 77%, of yields, respectively. The nanocatalyst was then investigated for its recyclability, which efficiently catalyze the reaction for four cycles without significant loss of catalytic activity. So, it can be concluded that this nanocatalyst acts better than the palladium homogeneous catalysts.

During an investigation of carbazole synthesis by means of a Pd(II)-catalyzed, one-pot reaction, Wu's group applied a procedure to *N*-aryl-2-aminopyridines **1** to achieve 9-(pyridin-2-yl)-9*H*-carbazoles **11** in moderate to high yields (Scheme 6).²⁹ The reaction involved *N*-aryl-2-aminopyridines and potassium aryltrifluoroborates in the presence of a Pd(OAc)₂ catalyst, AgOAc oxidant and benzoquinone (BQ) ligand. Using starting materials with different functional groups resulted in different ratios of products **10** and **11**, indicating the low selectivity of this reaction. The BQ ligand in collaboration with Ag(I) had an important role in not only the transmetalation but also reductive elimination.



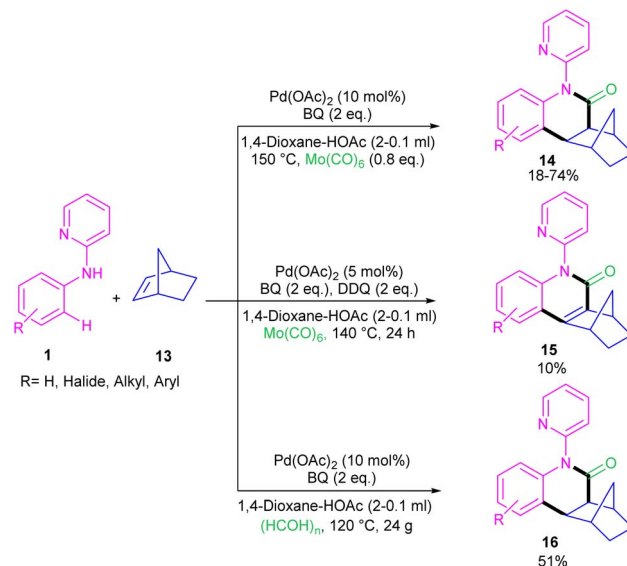
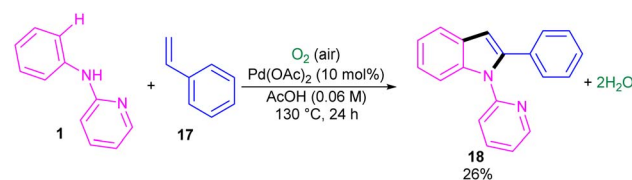
Scheme 5 NAP-Mg-Pd(0) catalyzed oxidative coupling of *N*-aryl-2-aminopyridines with alkynes.



Scheme 6 Pd(II)-catalyzed cross-coupling of *N*-phenylpyridin-2-amines with potassium aryltrifluoroborates.Scheme 7 Pd(II)-catalyzed C(sp²)-H pyridocarbonylation of *N*-aryl-2-aminopyridines.

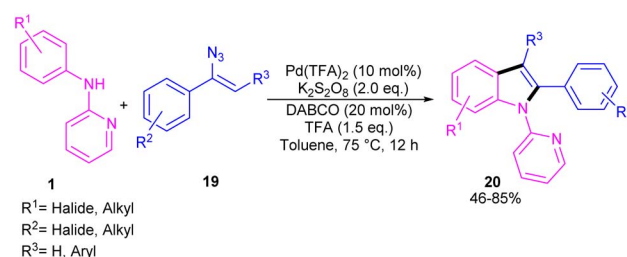
For preparing 11*H*-pyrido[2,1-*b*]quinazolin-11-ones **12**, Zhu *et al.* used Pd(OAc)₂ as a catalyst and CO gaseous to perform carbonylative intramolecular cyclization of *N*-aryl-2-aminopyridines **1** (Scheme 7).³⁰ The pyridyl nitrogen acted not only as a directing group for the metal but also as an intramolecular nucleophile. The reaction was found to proceed through intermediate **A**, **B** and **C**. The Pd(II) complex **A** was generated from the chelation of the nitrogen with the CO ligated Pd(II), which upon electrophilic cyclopalladation on the phenyl ring gave intermediate **B** via the C–H bond cleavage. After that, palladacycle **C** was formed via migratory insertion of a coordinated CO into the aryl–Pd bond, which after reductive elimination liberated the final product **12**. Later, Wu and co-workers reported the synthesis of 5-(pyridin-2-yl)-hexahydro-7,10-methanophenanthridin-6(5*H*)-ones from *N*-phenylpyridin-2-amine **1** and norbornene **13** as substrates using Pd(OAc)₂ as a catalyst and Mo(CO)₆ as a solid CO source (Scheme 8).³¹ Overall catalytic cycle involved Pd(II) insertion into the aromatic C–H bond, alkene coordination/insertion, CO coordination/insertion, and final reductive elimination. The carbonylation/cyclization reaction was also carried out by changing the BQ to DDQ as an oxidant or using paraformaldehyde as a CO source. However, DDQ can lead to the over oxidized product **15**.

The first report on the incorporation of olefins in intramolecular cyclization without the need of any additional directing group was performed by Maiti and his research team in 2014 (Scheme 9).³² *N*-Phenyl-2-aminopyridine **1** showed moderate reactivity in this reaction, resulting in 26% of yield of product **18**. In 2018, Wang, Cui and co-workers designed

Scheme 8 Pd(II)-catalyzed carbonylative C–H activation of *N*-aryl-2-pyridinamines with norbornene.

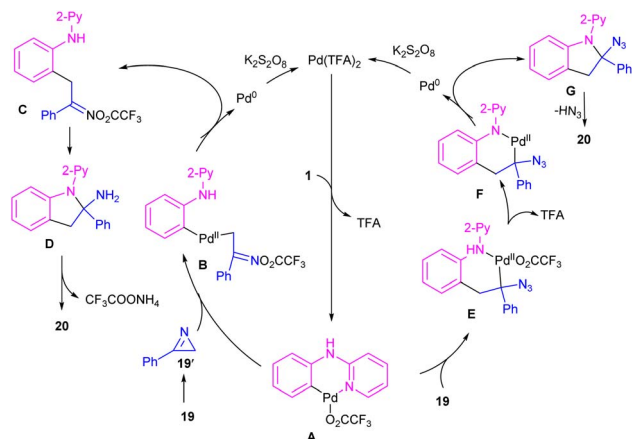
Scheme 9 Pd(II)-catalyzed cyclization of anilines with vinyl azides.

a strategy to achieve 2-arylindoles **20** via palladium-catalyzed reaction of *N*-phenyl-2-aminopyridine **1** with (1-azidovinyl)-benzene **19** (Scheme 10).³³ The mechanism started with a concerted metalation/deprotonation (CMD) process to access the palladacycle **A**. This intermediate could be moved through two pathways. In path I, the six-membered intermediate **A** underwent migratory insertion with vinyl azide **19**, and a subsequent elimination of TFA to yield another six-membered palladacycle **F**. Oxidative cyclization towards the indoline **G**, followed by the elimination of HN₃ furnished indole **20**. Meanwhile, K₂S₂O₈ oxidized Pd(0) to the active Pd(II) species to restart the next catalytic cycle. In path II, vinyl azide **19** transformed to 2*H*-azirine **19'** by the help of DABCO. Then, migratory insertion into palladacycle **A**, and subsequent reductive



Scheme 10 Pd(II)-catalyzed cyclization of anilines with vinyl azides.

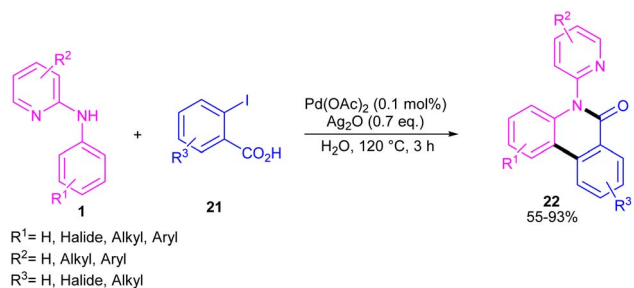




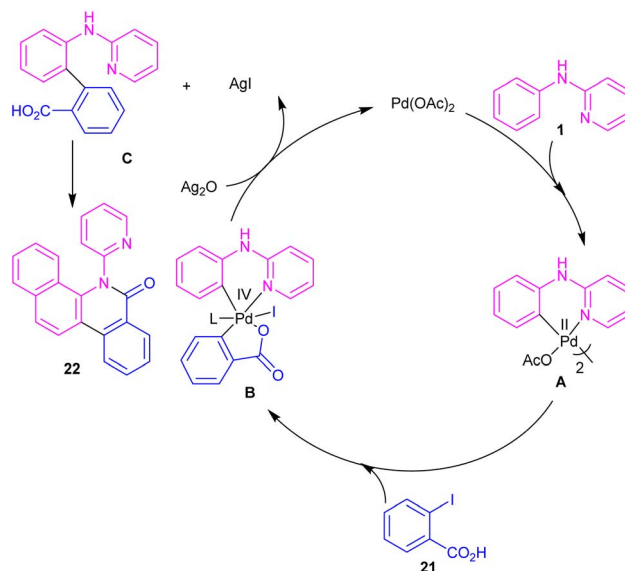
Scheme 11 Plausible mechanism for Pd(II)-catalyzed cyclization of anilines with vinyl azides.

elimination generated intermediate **C**. The generated Pd(0) species could be reoxidized to Pd(II) species. At last, **C** was subjected to an intramolecular nucleophilic addition to form intermediate **D**, which by further deamination delivered indole **20** (Scheme 11). It should be noted that intermediates **C** and **D** were determined by HRMS analysis, confirming the second pathway. In addition, KIE study ($K_H/K_D = 1.4$) indicated that the C–H bond cleavage is involved in the rate-determining step.

N-Aryl-2-aminopyridines **1** and 2-iodobenzoic acids **21** can react together in the presence of 0.1 mol% of Pd(OAc)₂ and 0.7 equiv. of Ag₂O in H₂O as a green solvent to construct phenanthridinone scaffolds **22** (Scheme 12).³⁴ The use of methyl 2-iodobenzoate and iodobenzene instead of 2-iodobenzoic acids did not result in any product, indicating the crucial role of the acid unit in the cyclization process. The isolation of the palladium intermediate **I** was successful, which in the reaction with 2-iodobenzoic acid led to the desired product in 91% yield. So, the reaction was found to move through the coordination of Pd(II) to the N-atom of *N*-aryl-2-aminopyridine, followed by C–H activation to form a six-membered palladacycle dimer **A**. In the next step, carboxylate-assisted oxidative addition to the metal center to render a Pd(IV) intermediate **B**. Then, reductive elimination of **B** in the presence of Ag(I) furnished the *ortho*-arylated product **C**. Further intramolecular acylation gave phenanthridinone **22** (Scheme 13).



Scheme 12 Pd(II)-catalyzed cyclization of *N*-aryl-2-aminopyridines with 2-iodobenzoic acids.

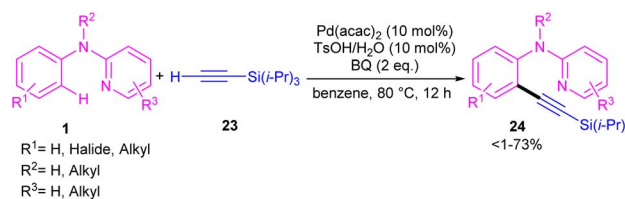


Scheme 13 Catalytic cycle for Pd(II)-catalyzed cyclization of *N*-aryl-2-aminopyridines with 2-iodobenzoic acids.

2.1.2. Functionalization

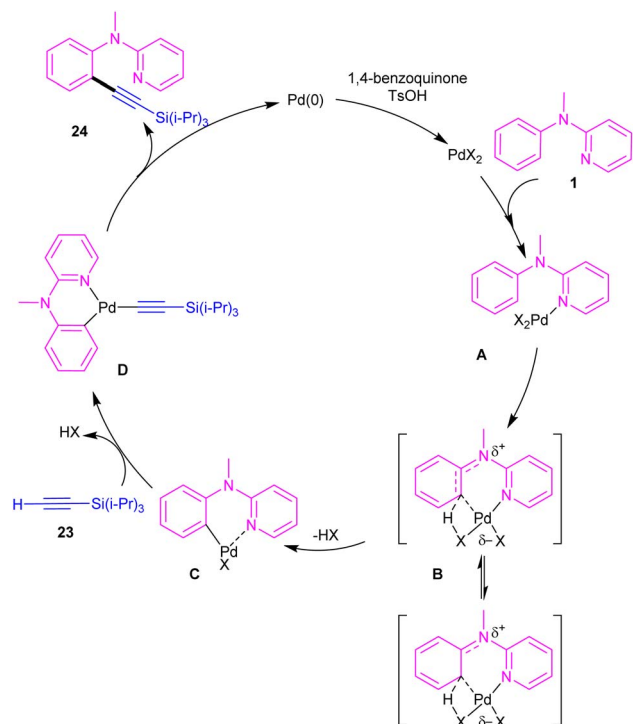
2.1.2.1. Alkynylation. Chang and co-workers investigated the reaction of *N*-aryl-2-aminopyridines **1** with (triisopropylsilyl) acetylene **23** in the presence of the palladium catalysts (Scheme 14).³⁵ Several palladium salts were explored [Pd(OAc)₂, Pd(acac)₂]; Pd(acac)₂ proved to be the most effective, in 100 mol% at 80 °C and in benzene as solvent. The KIE experiments indicated that C(sp²)–H bond cleavage is related to the rate-determining step. To determine the role of the nitrogen of *N*-aryl-2-aminopyridine in the catalytic pathway, the authors replaced *N*-aryl-2-aminopyridine with *N*-methyl-diphenylamine and 2-benzylpyridine as coupling reactants, resulting in no product. So, the reaction was proposed to carry out through intermediate **A**, followed by electrophilic metalation pathway to generate the arylpalladium π-complex **B**. It was found that the nitrogen linker between phenyl and 2-pyridyl moieties could stabilize **B** *via* equilibrating with **B'**. The conversion of **B** to the six-membered palladacycle **C**, and subsequent ligand exchange by acetylene afforded the arylpalladium acetylide intermediate **D**. The Pd(0) could be oxidized to Pd(II) in the presence of BQ and TsOH (Scheme 15).

2.1.2.2. Acylation. In 2023, Jiang, Ji and co-workers realized that PdCl₂ (15 mol%), Cu(OAc)₂ (1.1 equiv.), KI (20 mol%), and



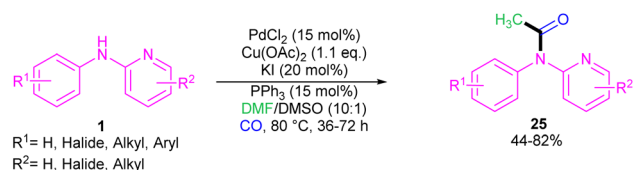
Scheme 14 Pd(II)-catalyzed reaction of *N*-aryl-2-aminopyridines with (triisopropylsilyl)acetylene.



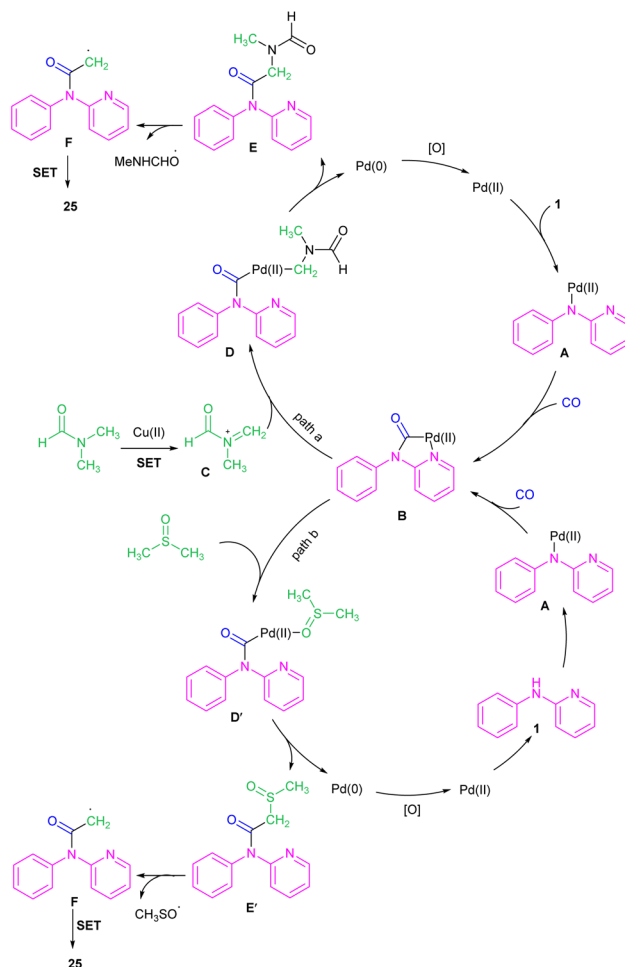


Scheme 15 Proposed mechanism for Pd(II)-catalyzed reaction of *N*-aryl-2-aminopyridines with (triisopropylsilyl)acetylene.

PPh_3 (15 mol%) with CO gaseous in DMF/DMSO at 80 °C constituted an efficient three-component system for the coupling of *N*-phenyl-2-aminopyridines with DMF and CO (Scheme 16).³⁶ In this protocol, DMF served as a methyl source and CO as a carbonyl source. When DMSO was used as a sole solvent, it could act as a methyl source. Although mechanistic studies using DMSO- d_6 showed that the methyl group in the product was originated from DMF not DMSO when the reaction performed in a mixture of both solvents, indicating DMF as a potential methyl source. The authors proposed a coupling mechanism in which Pd(0) inserted into the N–H bond of **1** to generate intermediate **A**, followed by the CO insertion to form intermediate **B**. In the meanwhile, DMF was oxidized to intermediate **C**, which then reacted with **B** to render intermediate **D**. The intermediate **E** was formed upon reductive elimination of **D**. Subsequent SET process in **E** afforded intermediate **F**, which was converted into product **25** via another SET step. Additionally, a carbonylative acetylation can also be carried out using DMSO as a methyl source. Upon the coordination of DMSO to intermediate **B**, intermediate **D'** was obtained, which



Scheme 16 Pd(II)-catalyzed acylation of *N*-phenyl-2-aminopyridines with DMF and CO.



Scheme 17 Rational mechanism for Pd(II)-catalyzed acylation of *N*-phenyl-2-aminopyridines with DMF and CO.

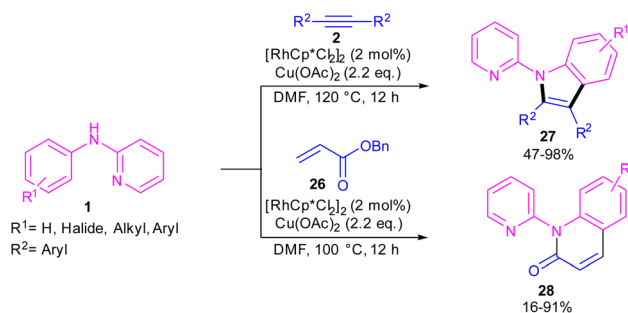
underwent reductive elimination to yield intermediate **E'**. After that, the conversion of **E'** to **F** via the C–S bond cleavage³⁷ and subsequent SET process delivered product **25** (Scheme 17).

2.2. Rh-catalyzed cross-coupling of *N*-aryl-2-aminopyridines

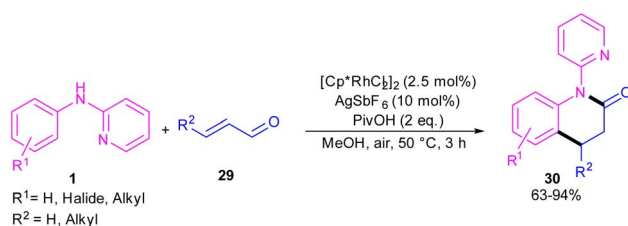
2.2.1. Annulation. In 2010, Li and co-workers reported an interesting method for producing *N*-(2-pyridyl)indoles **27** and *N*-(2-pyridyl)quinolones **28** through the annulation of two different reagents with *N*-aryl-2-aminopyridine **1** (Scheme 18).³⁸ For this purpose, they treated *N*-aryl-2-aminopyridine **1** with alkynes **2** in the presence of 2 mol% of $[\text{RhCp}^*\text{Cl}_2]_2$ to make *N*-(2-pyridyl)indoles **27** via (3 + 2)-cycloaddition process. In another transformation, 4 mol% of $[\text{RhCp}^*\text{Cl}_2]_2$ and acrylates **26** as coupling partners were used to perform (3 + 3)-cycloaddition with *N*-aryl-2-aminopyridine **1** towards the synthesis of *N*-(2-pyridyl)quinolones **28**. In addition, under these catalytic conditions, the reaction of styrene with *N*-aryl-2-aminopyridine led to mono- and disubstituted olefination products.

In 2017, Huang and co-workers developed Rh(III)-catalyzed $\text{C}(\text{sp}^2)\text{-H}$ functionalization/cyclization reaction of *N*-phenyl-2-aminopyridine and α,β -unsaturated aldehydes (Scheme 19).³⁹ A series of dihydroquinolinones were well synthesized from



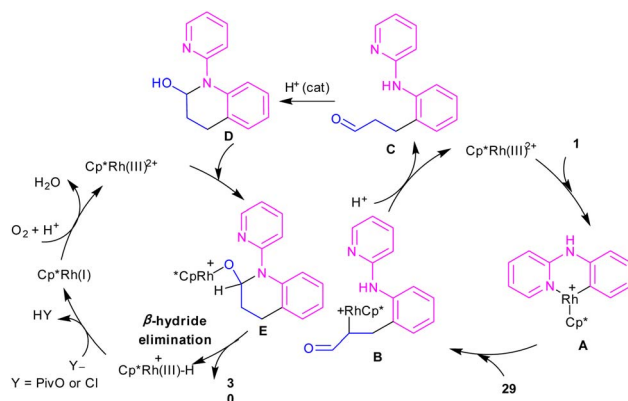


Scheme 18 Rh(III)-catalyzed C-annulation of *N*-aryl-2-aminopyridines with alkynes and acrylates.

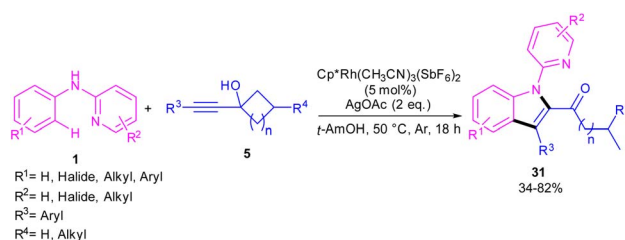


Scheme 19 Rh(III)-catalyzed C–H functionalization/cyclization reaction of *N*-arylpyridin-2-amines with α,β -unsaturated aldehydes.

both electron-rich and electron-poor *N*-aryl-2-aminopyridine substrates. According to the rhodium catalytic cycle in Scheme 20, pyridine-directed Rh(III) insertion in the $\alpha\text{-C}(\text{sp}^2)\text{-H}$ bond of *N*-aryl-2-aminopyridine **1** to produce a six-membered rhodacycle **A**. Then, propenal **29** inserted into **A** to form intermediate **B**, which was protonated to generate intermediate **C**. Acid-catalyzed intramolecular nucleophilic addition of the amine onto the carbonyl group to yield α -hydroxyl tetrahydroquinoline **D**. Afterward, through a ligand exchange between $\text{Cp}^*\text{Rh}(\text{III})^{2+}$ and **D**, a rhodium intermediate **E** was obtained, which underwent β -hydride elimination to afford the tetrahydroquinoline product **30** and $\text{Cp}^*\text{Rh}(\text{III})\text{-H}$. The interaction of the anion Y^- and $\text{Cp}^*\text{Rh}(\text{III})\text{-H}$ resulted in the loss of a HY molecule, followed by reductive elimination to Cp^*Rh and subsequent oxidation to the catalytically active $\text{Cp}^*\text{Rh}^{2+}$ species.

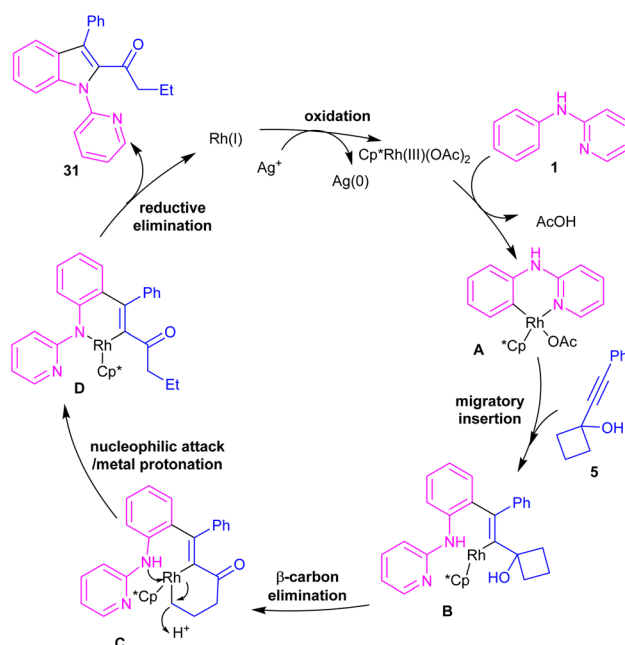


Scheme 20 Rh(III)-catalyzed C–H functionalization/cyclization reaction of *N*-arylpyridin-2-amines with α,β -unsaturated aldehydes.



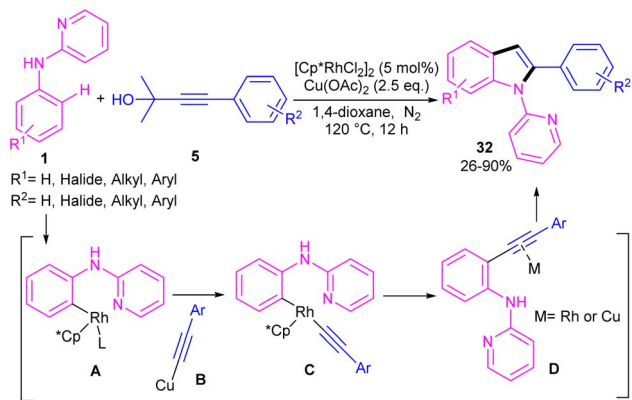
Scheme 21 Rh(III)-catalyzed cross-coupling/cyclization between *N*-aryl-2-pyridinamines and propargyl cycloalkanols.

In the same year, Zeng's research team developed a rhodium catalytic strategy for the cross-coupling/cyclization between *N*-aryl-2-pyridinamines **1** and propargylic cycloalkanols **5** (Scheme 21).⁴⁰ A series of 1,2,3-trisubstituted indoles **31** were synthesized in moderate to high yields. Evaluating various transition metals, including $\text{Pd}(\text{OAc})_2$, $\text{Cp}^*\text{Co}(\text{CO})\text{I}_2$, (*p*-cymene RuCl_2), $[\text{Cp}^*\text{IrCl}_2]_2$, RhCl_3 , $[\text{Cp}^*\text{RhCl}_2]_2$ and $\text{Cp}^*\text{Rh}(\text{CH}_3\text{CN})_3(\text{SbF}_6)_2$ showed that only rhodium complexes have catalytic activity in this transformations, while others remained ineffective. A reasonable rhodium catalytic cycle involved the C–H activation of substrate **1** with the Rh(III) catalyst to form a six-membered rhodacycle **A** via a CMD process. Next, the migratory insertion of **5** to Rh(III) complex **A** afforded Rh(III) species **B**, which under a β -carbon elimination gave rhodacycle **C**. Intramolecular nucleophilic attack of the N-atom to Rh(III) and subsequent protonation rendered a Rh(III) complex **D**, followed by reductive elimination to yield 1,2,3-trisubstituted indole **31**. The generated Rh(I) was then oxidized to the catalytically active Rh(III) species (Scheme 22). The synthetic



Scheme 22 Possible mechanism of Rh(III)-catalyzed cross-coupling/cyclization between *N*-aryl-2-pyridinamines and propargyl cycloalkanols.

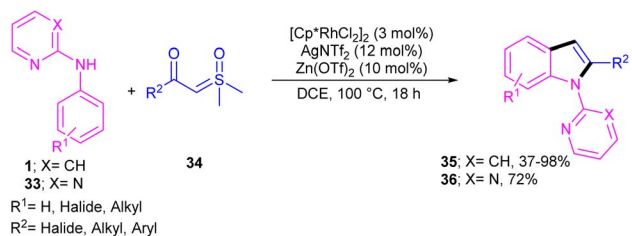




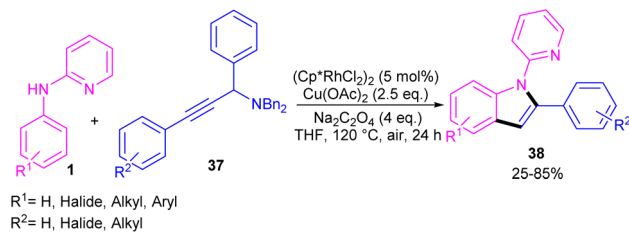
Scheme 23 Rh(III)-catalyzed annulation of *N*-phenyl 2-aminopyridine and propargylic alcohols.

application of this method was showed by the introduction of a carbonyl methylene group at the C7-position of indole and also the reduction of ketone to the alcohol moiety.

Propargylic alcohols can be a practical coupling partner in the reaction with *N*-aryl-2-aminopyridines to assemble indole derivatives (Scheme 23).⁴¹ 5 mol% of Rh(III) and 2.5 equiv. of Cu(II) constitute an efficient catalytic system for the C–H activation and cascade annulation reaction. In this regard, *ortho* C(sp²)–H cleavage of **1** gave ruthenacycle **A**, which was then coordinated with the alkynyl copper species **B** to form an alkynyl rhodium **C** through transmetalation. Next, reductive elimination and subsequent annulation *via* nucleophilic attack of the amino group to the activated alkynyl moiety occurred in the presence of a Lewis acid (Rh or Cu salt) to deliver product **32**. The generated Rh(I) was oxidized by Cu(II) to the active Rh(III) species to fulfill the catalytic cycle. None of metal catalysts including Ni(OAc)₂·4H₂O, Co(OAc)₂·4H₂O, [RuCl₂(*p*-cymene)]₂, and Pd(OAc)₂ were workable. The same rhodium catalyst can also catalyze the annulation of *N*-aryl-2-aminopyridines **1** and *N*-aryl-2-aminopyrimidine **33** with sulfoxonium ylides **34** to provide indoles **35**, **36** in up to excellent yields (Scheme 24).⁴² The indole synthesis involved C–H activation, coordination/insertion, and reductive elimination. The DMSO and H₂O molecules were the only byproducts of this reaction. A similar rhodium catalytic system was reported for the reaction of *N*-aryl-2-aminopyridines **1** with propargylic amines **37** to assemble the indole products **38** (Scheme 25).⁴³ A reaction mechanism similar to propargylic alcohols was suggested for this



Scheme 24 Rh(III)-catalyzed annulation of *N*-phenyl 2-aminopyridine and sulfoxonium ylides.

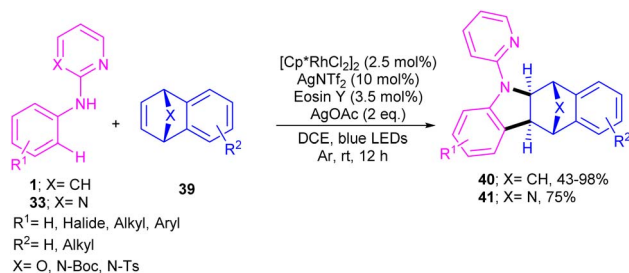


Scheme 25 Rh(III)-catalyzed annulation of *N*-phenyl 2-aminopyridine and propargylic amines.

transformation, involving Rh-catalyzed C–H activation, alkyne insertion, and Lewis acid-promoted nucleophilic attack of the amino group to the activated alkynyl moiety towards intramolecular cyclization.

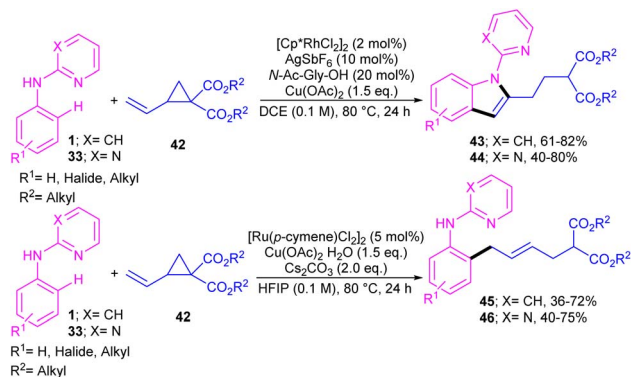
The cooperation of a rhodium catalysis and a photocatalysis can provide an efficient system for synthesizing a new library of bridged tetrahydro benzocarbazole scaffolds **40**, **41** (Scheme 26).⁴⁴ Various oxa- and aza-bicyclic alkenes were tolerated smoothly in the (2 + 3)-annulation reaction with *N*-aryl 2-aminopyridines **1** leading to bridged oxa-, aza-tetrahydro benzocarbazoles. The structure of bicyclic motif was intact in this reaction. Further aromatization under acidic conditions can provide the corresponding benzo[*b*]carbazoles *via* a ring-opening/hydration step. The method has the advantages of low catalyst loading, mild reaction conditions, broad functional groups tolerance and gram-scale synthesis. In addition, the removal of the directing group pyridine, acylation and Ullmann C–N coupling under copper catalysis were also carried out in this work.

A series of *N*-phenyl 2-aminopyridines **1** and *N*-phenyl 2-aminopyrimidines **33** were investigated in the reaction with electron-deficient cyclopropanes **42** under metal catalysis systems (Scheme 27).⁴⁵ Interestingly, when *N*-phenyl 2-aminopyridine used as a substrate, open-chain aniline products were obtained under ruthenium catalytic conditions. While these substrates did not reactive in the presence of a rhodium catalyst. Unlike, *N*-phenyl 2-aminopyrimidines were well tolerated in not only ruthenium-catalyzed reaction with cyclopropanes towards aniline products but also in rhodium-catalyzed annulation reaction with cyclopropanes towards indole frameworks. However, the replacement of NH-phenyl moiety with *O*-phenyl or *S*-phenyl group in the pyridine and pyrimidine substrates

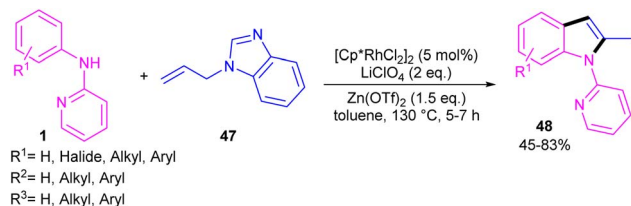


Scheme 26 Rh(III)-catalyzed C–H annulation of aromatic amines with bicyclic alkenes.





Scheme 27 Catalyst-controlled chemodivergent approach to access C2-substituted indoles and aniline derivatives.



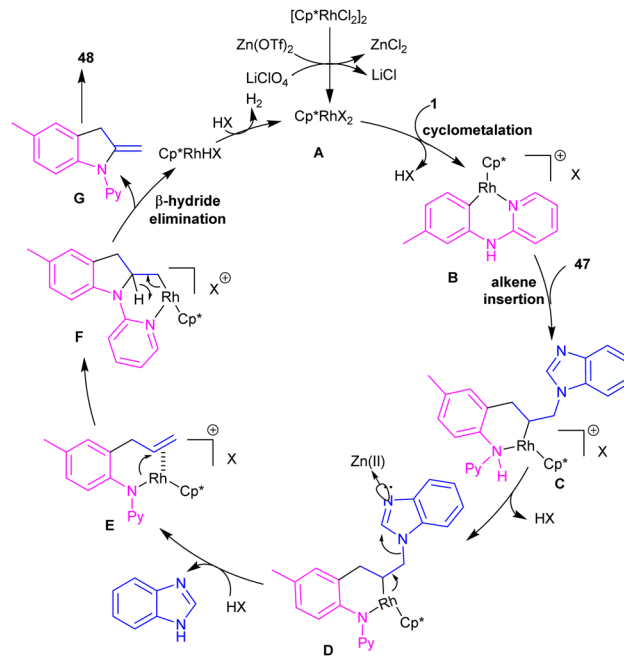
Scheme 28 Rh(III)-catalyzed (3 + 2)-annulation of *N*-phenyl 2-aminopyridine and *N*-allylbenzimidazole.

did not yield any products, indicating the important role of the nitrogen as a chelating group for the formation of the metal complexes.

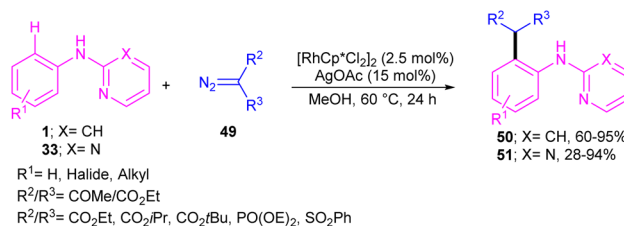
2-Methylindole derivatives can be achieved from the (3 + 2)-annulation of *N*-phenyl 2-aminopyridines and *N*-allylbenzimidazoles (Scheme 28).⁴⁶ The method involved the cleavage of C–N bond of *N*-allylbenzimidazole to act as a 2C synthon participated in the intramolecular (3 + 2)-cycloaddition with *N*-phenyl 2-aminopyridines. Radical scavenger experiments by TEMPO and BHT demonstrated a non-radical pathway. The catalytic cycle involved irreversible cyclometalation of the active catalyst **A** with *N*-(*p*-tolyl)pyridine-2-amine **1**, followed by migratory insertion of alkene **47** into the Rh–C bond. Next, the removal of benzimidazole gave intermediate **E**, followed by the addition of alkene to the Rh–N bond to form intermediate **F**. The β -hydride elimination of **F**, and subsequent aromatization delivered product **48** (Scheme 29). The utility of this method was demonstrated by removal of the pyridyl group, bromination, and acetylation reactions of indole as well as the gram-scale synthesis.

2.2.2. Functionalization

2.2.2.1. Alkylation. Kim and co-workers reported the cross-coupling of *N*-aryl-2-aminopyridines and *N*-aryl-2-aminopyrimidines with diazo compounds in moderate to excellent chemical yields in the presence of [RhCp*Cl₂]₂ (2.5 mol%) and AgOAc (15 mol%) in methanol (Scheme 30).⁴⁷ Diazo malonates as coupling partners gave the alkylation products, while the indole products were isolated using diazo acetoacetates. In every case of alkylation, only monoalkylation



Scheme 29 Catalytic cycle for Rh(III)-catalyzed (3 + 2)-annulation of *N*-phenyl 2-aminopyridine and *N*-allylbenzimidazole.

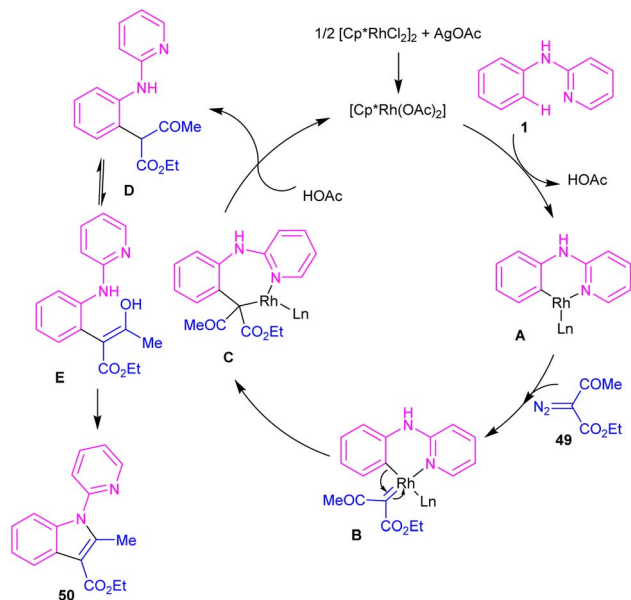


Scheme 30 Rh(III)-catalyzed alkylation of *N*-phenyl 2-aminopyridine with diazo compounds.

product was observed, and it occurred exclusively in the C2-position. Late-stage functionalizations of the indole compounds at the C7-position, including alkylation, cyanation and amidation were also performed in this work. The mechanism of the reaction involved the generation of a six-membered rhodacycle **A** from **1** and the Rh(III), followed by the coordination of α -diazo compound **49** along with release of N₂ to form the metal-carbenoid intermediate **B**. Migratory insertion in **B** rendered the seven-membered rhodacycle **C**, which was protonated to generate the *ortho*-alkylated product **D** and the reactive Rh(III) species. On the other hand, through a keto-enol tautomerization of **D**, intermediate **E** was obtained, which was then subjected to dehydration to afford indole **50** (Scheme 31).

2.2.2.2. Thiolation. In 2017, Yang and his team realized that [Cp*RhCl₂]₂, AgOTf and Ag₂CO₃ in toluene at 130 °C can constitute an efficient catalytic system for the coupling of *N*-aryl-2-pyridinamines **1** or 2-phenoxy-pyridines **52** with aryl/alkyl disulfides **53** (Scheme 32).⁴⁸ This work presented a method for the selective monothiolation of *N*-aryl-2-pyridinamines and 2-phenoxy-pyridines. Several mechanistic reactions were carried

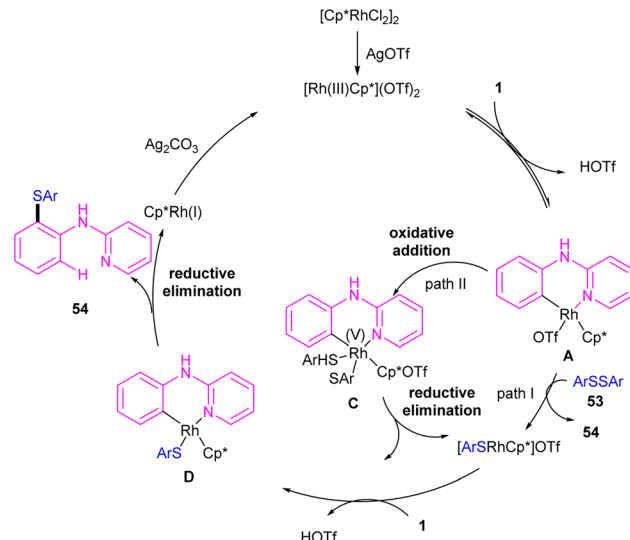




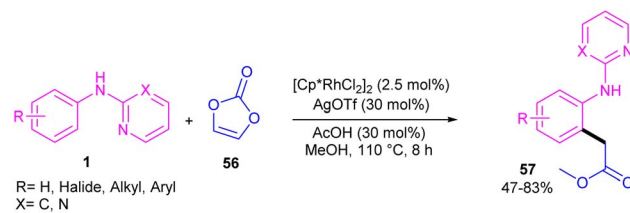
Scheme 31 Plausible catalytic pathway for Rh(III)-catalyzed alkylation of *N*-phenyl 2-aminopyridine with diazo compounds.



Scheme 32 Rh(III)-catalyzed annulation of *N*-aryl-2-pyridinamines with disulfides.



Scheme 33 Credible mechanism for Rh(III)-catalyzed annulation of *N*-aryl-2-pyridinamines with disulfides.



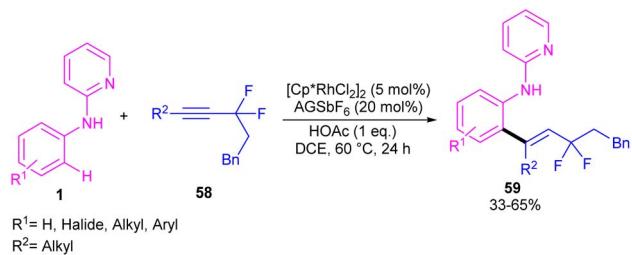
Scheme 34 Rh(III)-catalyzed C-H carboxymethylation of *N*-aryl-2-aminopyridines with vinylene carbonate.

out to reveal the real mechanism; in a competitive reaction, electron-donating groups on the benzene ring of *N*-aryl-2-pyridinamines showed higher reactivity. Deuterium labeling experiments also confirmed the reversibility of C-H activation and the involvement of it in rate-determining step. Therefore, a six-membered rhodacyclic intermediate **A** was proposed to generate, which could be transformed to the rhodium(III) intermediate **C** through the oxidative addition of disulfide **53**. The final product **54** was obtained *via* either direct reductive elimination of **C**, or from the reductive elimination of the rhodacyclic intermediate **D**. It should be noted that intermediate **D** could be obtained *via* the second C-H activation **1** and **B** (Scheme 33).

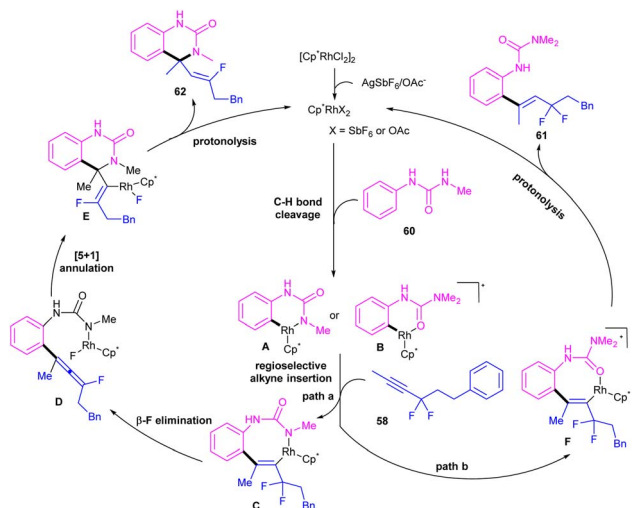
Regioselective C-H carboxymethylation of *N*-aryl 2-aminopyridines **1** with vinylene carbonate **56** can be carried out in the presence of a rhodium catalyst (Scheme 34).⁴⁹ The transformation was not successful using other metal catalysts, such as ruthenium and iridium complexes. The catalytic procedure involved C-H activation, the vinylene carbonate insertion, and 1,2-Rh-C migration/decarboxylation. The easy removal of pyridine directing group was also possible under basic conditions. In addition, the large-scale synthesis the product (1.02 g, 70% yield) and the hydrolysis of the ester to acid group showed the utility of this method.

2.2.2.3. Alkenylation. A remarkable rhodium catalyzed C-H alkenylation of *N*-aryl-2-aminopyridine **1** with *gem*-difluoromethylene alkynes **58** was explored by Yi *et al.* (Scheme 35).⁵⁰ Fluorine functional groups can affect the coordination mode of the Rh(III) catalyst binding to the directing group, leading to difluorinated 2-alkenyl arylureas and 3,4-dihydroquinazolin-2(1*H*)-ones with an α -quaternary carbon center and a monofluoroalkenyl motif. Deuterium-labeling and KIE experiments indicated the reversibility of the C-H activation and non-involvement of the C-H activation in the rate-determining step. The authors assumed arylurea **60** as a substrate to design a plausible mechanism. As shown in Scheme 36, the active cationic Cp*Rh(III) catalyst coordinated with the arylurea substrate **60** followed by the *ortho* C-H bond activation to generate the six-membered rhodacycle **A** or **B**. In path I, intermediate **A** moved through a regioselective migratory insertion with alkyne **58**, followed by β -F elimination to form a fluoroallene intermediate **D**. Intramolecular (5 + 1)-cycloaddition in **D** gave the 3,4-dihydroquinazolin-2(1*H*)-one skeleton **E**, which under protonolysis delivered product **61** and the active Rh(III) species. In path II, rhodacycle **B** underwent an alkyne insertion to afford intermediate **F**, which by further protonolysis furnished product **62**.



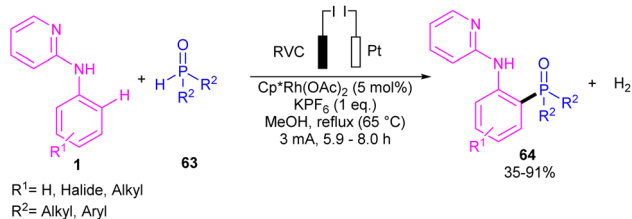


Scheme 35 Rh(III)-catalyzed C–H alkenylation of *N*-pyridylanilines and *gem*-difluoromethylene alkynes.

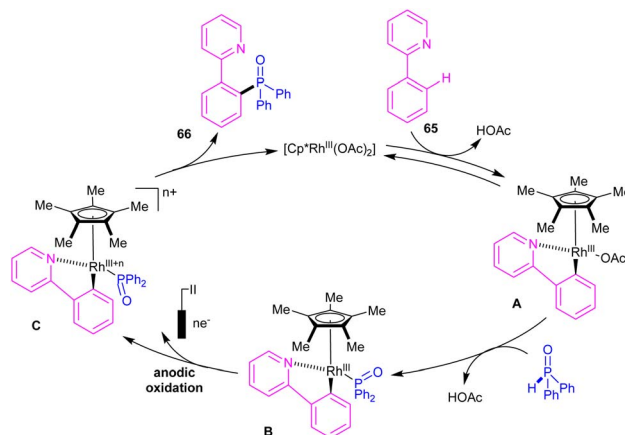


Scheme 36 Plausible mechanism for Rh(III)-catalyzed C–H alkenylation with *N*-pyridylanilines and *gem*-difluoromethylene alkynes.

2.2.2.4. Phosphorylation. Phosphorylation of *N*-aryl-2-aminopyridines with a wide range of phosphorous reagents was reported under electrochemical conditions (Scheme 37).⁵¹ This method presented a silver-free Rh-catalyzed coupling reaction between C–H and P–H bonds. A series of triaryl/alkylphosphine oxides **64** were obtained in moderate to excellent yields. In addition to *N*-aryl-2-aminopyridine, various aryl substrates such as 2-phenylpyridine, 1-phenylpyrazole and 1-methyl-5-phenyl-1,3-dihydro-2*H*-benzo[*e*][1,4]diazepin-2-one were also incorporated in the reaction with *H*-phosphonates. The authors designed a rational mechanism using 2-phenylpyridine **65** and diphenylphosphine oxide **63** as coupling



Scheme 37 Rh(III)-catalyzed C–H phosphorylation of *N*-aryl-2-aminopyridines with phosphorous reagents.

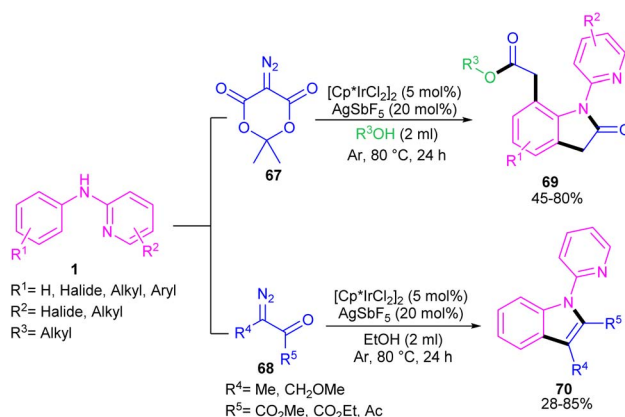


Scheme 38 Electrochemical cycle for Rh(III)-catalyzed C–H phosphorylation of *N*-aryl-2-aminopyridines with phosphorous reagents.

partners. The reaction was initiated by the activation of C(sp²)–H bond of *N*-aryl-2-aminopyridines by the metal to form rhodacycle **A**, which exchanged a ligand with **65** to yield a more oxidizable organometallic complex **B**. Next, reductive elimination of **B** by anodic oxidation afforded product **66** and either Rh(III) or Rh(II) species depending on the oxidation state of **C**. H₂ molecular was produced by the reduction of protons at the cathode (Scheme 38).

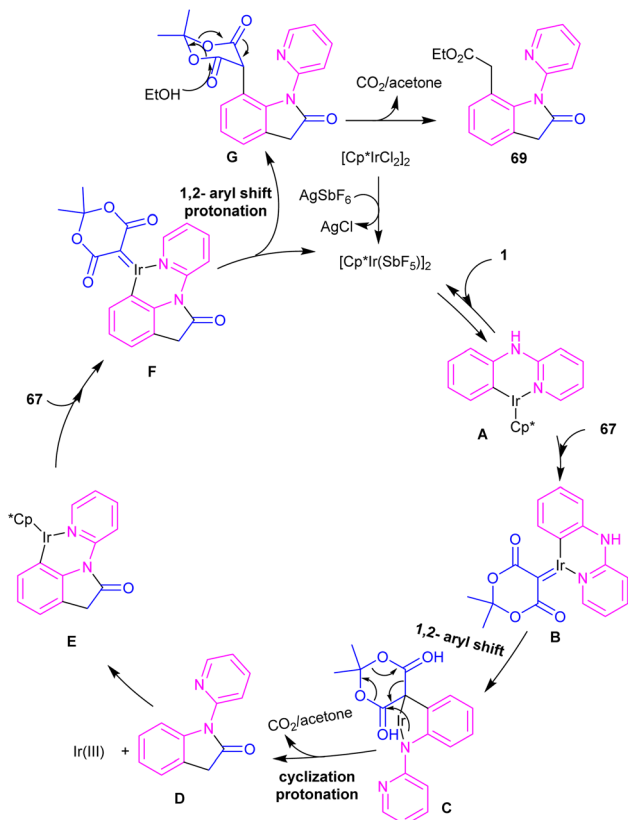
2.3. Ir-catalyzed cross-coupling of *N*-aryl-2-aminopyridines

2.3.1. Annulation. Zeng and co-workers established an iridium(III) catalysis system for the annulation/functionalization of *N*-aryl-2-pyridinamines with diazo Meldrum's acid (Scheme 39).⁵² Various diazo compounds were investigated in the reaction with *N*-aryl-2-pyridinamines, in which 1,3-diketo-2-diazo compounds, and 1,3-ketoester-2-diazo compounds led to the corresponding indoles *via* mono selective *ortho* C–H activation. However, 1,3-diester-2-diazo compound and ethyl diazoacetate did not give any product. A possible mechanism was proposed for this carbenoid insertion/cyclization reaction, involving *N*-pyridyl coordination of **1** to the Ir(III), and



Scheme 39 Ir(III)-catalyzed annulation of *N*-aryl-2-pyridinamines with diazo Meldrum's acid.

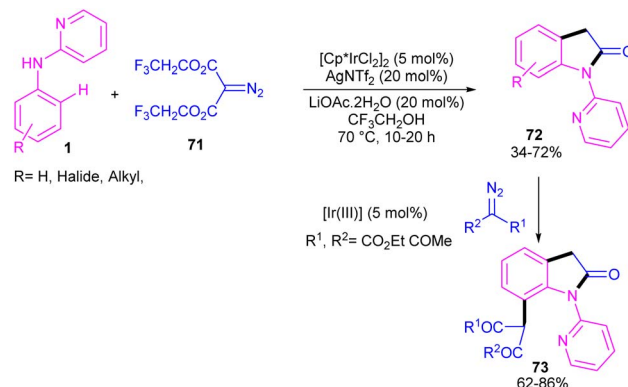




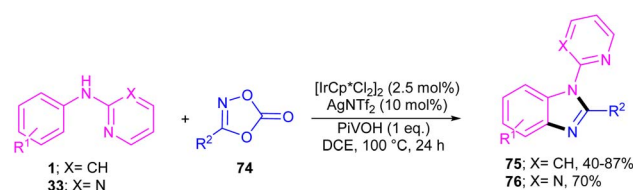
Scheme 40 Possible mechanism for Ir(III)-catalyzed annulation of *N*-aryl-2-pyridinamines with diazo Meldrum's acid.

subsequent phenyl C–H activation to form a six-membered Ir(III) complex **A** via a CMD process. Next, diazo compound **67** coordinated to the metal center of **A**, followed by denitrogenation to yield Ir–carbene **B**. After that, **B** underwent 1,2-aryl migratory insertion and cyclization/deprotonation to form *N*-(2-pyridyl)-2-indolone **D**. Finally, pyridyl-assisted the C(sp²)-H bond carbene insertion to obtain intermediate **G**, which nucleophilically attacked by an alcohol to provide the 7-substituted-2-oxindoles **69** with the release of acetone and CO₂ (Scheme 40). Another work on the synthesis of oxindoles starting from *N*-phenyl-2-aminopyridine **1** with bis(2,2,2-trifluoroethyl) 2-diazomalonate **71** was described in the same year (Scheme 41).⁵³ In this method, the same iridium(III) catalyst used by Zeng, could catalyze the assembly of oxindoles and 7-substituted-2-oxindoles. The general mechanism involved pyridyl-directed C–H activation, interaction of **71** with the Ir center to form iridium–carbene bond, migratory insertion, reductive elimination and the removal of CF₃CH₂H and CO₂.

The first C–H activation and intermolecular coupling reaction access to benzimidazoles was reported by the Li group in 2017 (Scheme 42).⁵⁴ The authors highlighted the importance of both [Cp*IrCl₂]₂ and a silver additive for this reaction. The reaction of *N*-aryl-2-pyridinamines and dioxazolones involved a redox-neutral mechanism and CO₂ and H₂O were the only byproducts. First, nitrogen-assisted C–H activation of **1** with the metal produced complex **A**, which further coordinated with **74**

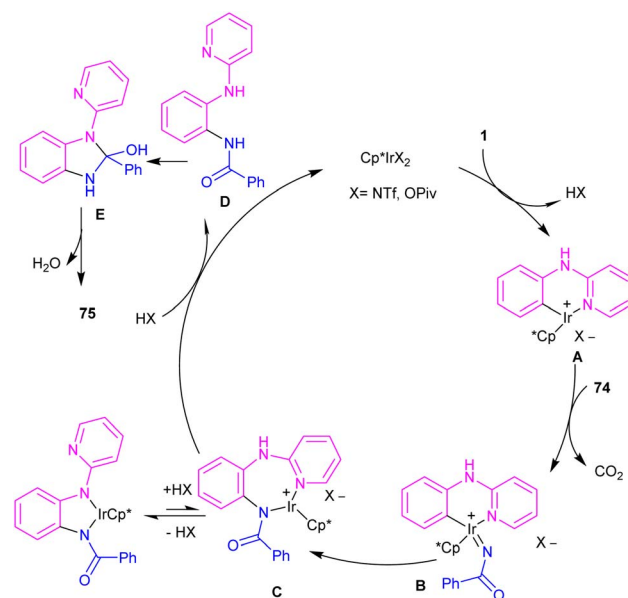


Scheme 41 Ir(III)-catalyzed annulation of *N*-phenyl-2-aminopyridine with bis(2,2,2-trifluoroethyl) 2-diazomalonate.



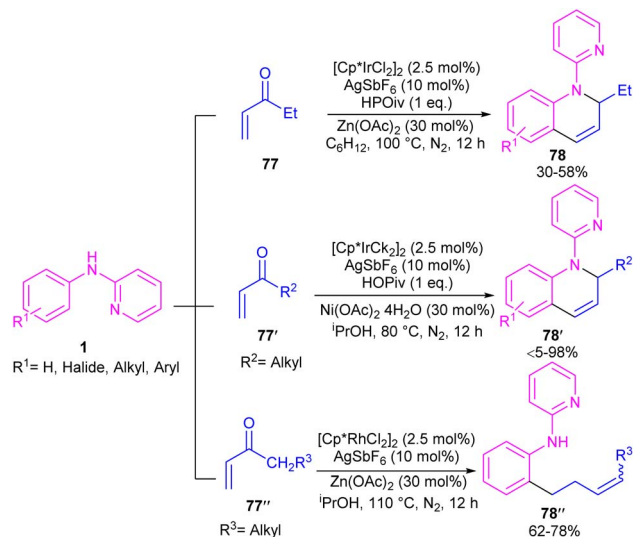
Scheme 42 Ir(III)-catalyzed C–H activation and amidation of aniline derivatives.

to yield a nitrenoid species **B** with the emission of CO₂. Migratory insertion of nitrenoid into the Ir–aryl bond led to amidate **C**, which was protonated into an amidated intermediate **D**, together with regeneration of the Cp*Ir(III). Eventually, PivOH or Cp*Ir(III)-mediated intramolecular nucleophilic attack at the acyl group, followed by dehydration to furnish product **75** (Scheme 43).



Scheme 43 Rational mechanism for Ir(III)-catalyzed C–H activation and amidation of aniline derivatives.

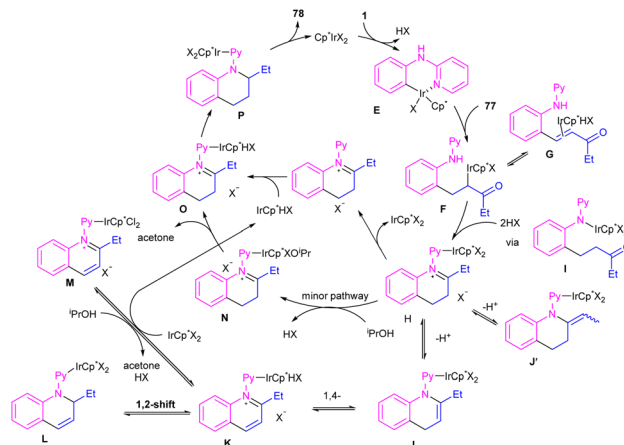




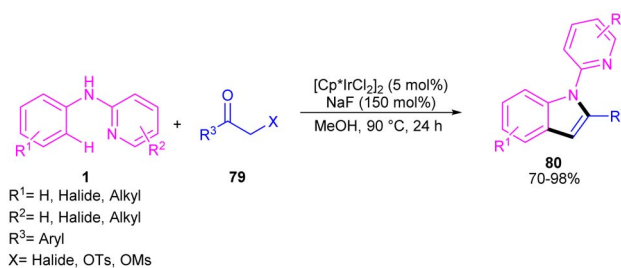
Scheme 44 Ir(III) and Rh(III)-catalyzed annulation and alkylation of *N*-aryl 2-aminopyridines with enones, respectively.

By controlling of the type of the transition metal catalyst, Li co-workers were able to isolate two different products from the reaction of *N*-aryl 2-aminopyridines with enones (Scheme 44).⁵⁵ In their work, iridium-catalyzed reaction of *N*-aryl-2-aminopyridines and enones can produce tetra- or dihydroquinoline products, while a rhodium catalysis system including these two starting materials led to the alkylation products. It should be noted that using different iridium catalytic conditions could also lead to the alkylation products. It was shown that iridium catalyze the reaction through intermediate **A**, which under acidic media could be converted to intermediate **B**. Subsequent transfer hydrogenation in **B** provided the cyclized products. Whereas, intermediate **A** directly afforded the alkylation product **78''** under rhodium catalysis. A plausible mechanism was proposed for generating 1,2-dihydroquinolines. First, after the generation of iridacycle **E** via C–H activation of aniline **1** by metal, coordination and insertion of enone **77** into the Ir–Ar bond occurred to obtain the Ir(III) alkyl complex **F** in equilibrium with hydride **G**. After that, **F** was protonated and cyclized in the presence of Lewis acid Zn(II) or Ni(II). The obtained iminium ion **H** was then subjected to a ligand exchange with isopropoxide and subsequent β-H elimination to produce the Ir(III) hydride **O**. Next hydride attack to **O** provided amine **P**, which was converted to product **78** after a ligand dissociation. However, in the major pathway, reversible deprotonation of **H** gave enamines **J** or **J'**. Intermediate **J** can be converted to **K**, and **L** via reversible 1,4- and 1,2-hydride insertion. Through a ligand dissociation–association in the metal center of **H** and **K**, intermediate **M** was obtained, which can be reduced by *i*PrOH into **H**. Finally, disproportionation of a dihydroquinoline (**J/L**), and subsequent reduction of the quinolinium **K** delivered product **78** (Scheme 45).

The indole synthesis can be achieved from the annulation of *N*-aryl-2-aminopyridines **1** with α-chloro ketones **79** under



Scheme 45 Plausible mechanism for Ir(III)-catalyzed annulation of *N*-aryl 2-aminopyridines with enones.



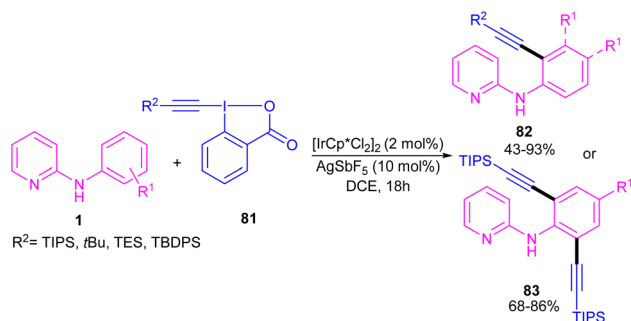
Scheme 46 Ir(III)-catalyzed C–H annulation of *N*-phenyl-2-aminopyridines with α-chloro ketones.

iridium catalysis (Scheme 46).⁵⁶ The reaction was not proceeded in the presence of [Ru(*p*-cymene)Cl₂]₂ and Cp*Co(CO)I₂, while led to 15% of chemical yield using [RhCp*Cl₂]₂. The transformation did not significantly influence by the electronic properties of substituents at the both benzene and pyridyl ring of *N*-aryl-2-aminopyridines, where the all products were obtained in high to excellent yields. Moreover, a wide range of α-chloro ketones with aryl, naphthyl, and heteroaryl moieties were compatible.

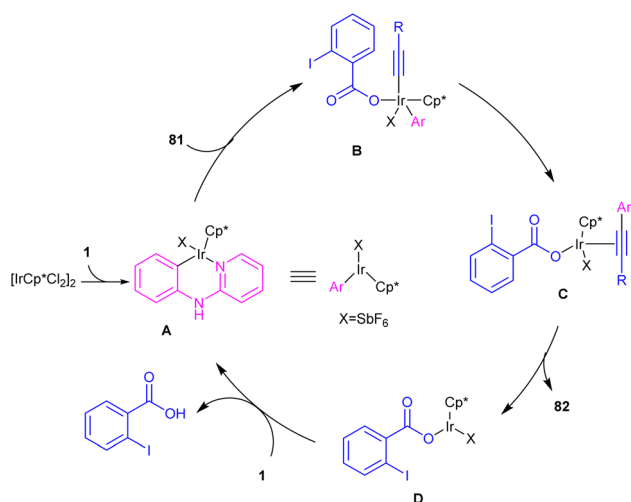
2.3.2. Functionalization

2.3.2.1. Alkenylation. In 2016, *N*-phenyl-2-aminopyridines were investigated for the alkylation in the presence of a hypervalent iodine alkyne (TIPS-EBX) as a coupling partner (Scheme 47).⁵⁷ Iridium(III) could efficiently catalyze the *ortho*-C–H alkylation of *N*-phenyl-2-aminopyridines. Selectivity of mono alkylation can be better achieved using TIPS-EBX compared to other alkyne sources. However, *ortho*- and *meta*-substituted benzene ring led to selective mono-alkynylation, while *para*-substituted benzene gave dialkynylated products. The reaction mechanism involved the formation of an active cationic Ir(III) species from the ligand exchange between [IrCp*Cl₂]₂ and AgSbF₆, followed by the coordination of metal center with **1** to produce a six-membered iridacycle **A**. Oxidative addition of R-EBX **81** to **A** gave Ir(V) intermediate **B**, which under reductive elimination afforded Ir(III) alkyne **C**. Another C–C





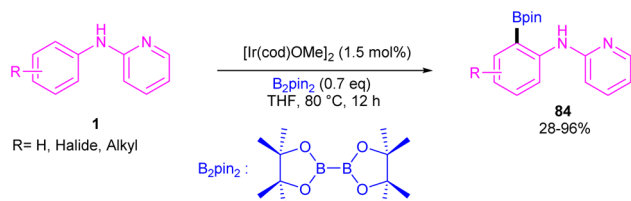
Scheme 47 Ir(III)-catalyzed C–H alkynylation of *N*-phenyl-2-aminopyridines.



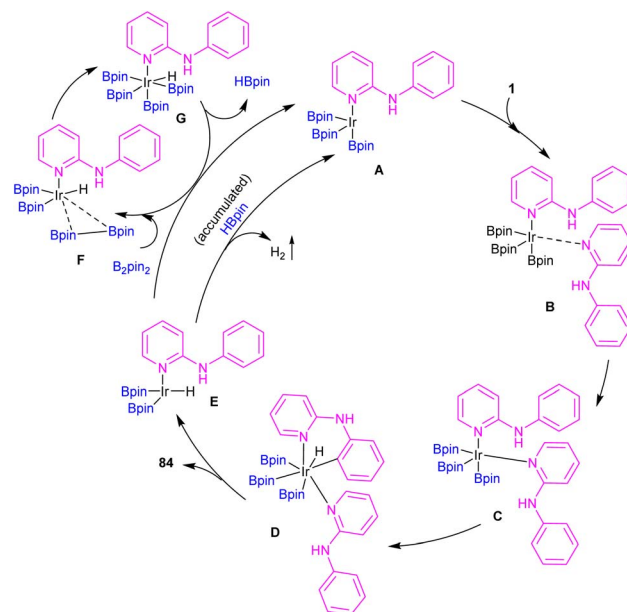
Scheme 48 Catalytic cycle for Ir(III)-catalyzed C–H alkynylation of *N*-phenyl-2-aminopyridines.

reductive elimination led to Rh(III) benzoic species **D** and the coupling product **82**. Subsequently C–H activation of **1** resulted in the active iridacycle **A** and 2-iodobenzoic acid (Scheme 48). KIE experiment suggested the C–H activation is the rate-determining step.

2.3.2.2. Borylation. An iridium catalysis system for the *ortho*-selective borylation of 2-anilino-2-pyridines and 2-phenoxy-2-pyridines was developed by Chattopadhyay and his team in 2022 (Scheme 49).⁵⁸ By decreasing the temperature, the authors were able to control the mono-borylation over di-borylation reaction. So, in lower temperatures mono-borylated products were the



Scheme 49 Ir(III)-catalyzed C–H borylation of 2-anilino-2-pyridines and 2-phenoxy-2-pyridines.



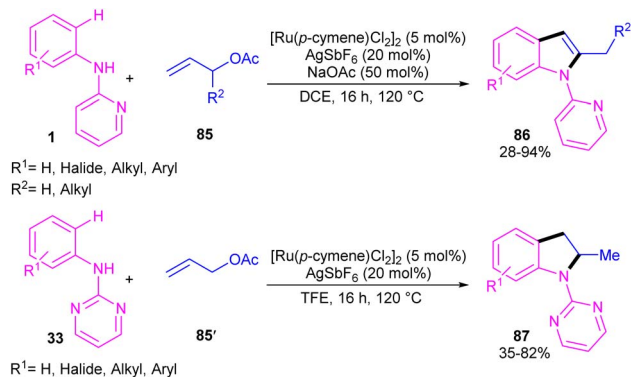
Scheme 50 Catalytic cycle for Ir(III)-catalyzed C–H borylation of 2-anilino-2-pyridines and 2-phenoxy-2-pyridines.

main products, whereas the higher temperatures were suitable for the di-borylation reaction. The borylated products were isolated up to excellent yields. Besides, other arenes, including benzylamines/piperazines/morpholines/pyrrolidine/piperidines/azepanes, α -amino acids, aminophenylethanes were participated in this catalytic system. According to KIE and DFT studies, a rational catalytic cycle was suggested involving a key iridium–boryl intermediate. Two molecules of substrate **1** coordinated with iridium to give intermediate **A**, which led to the iridium complex $\text{Ir}(\text{1})_2(\text{Bpin})_3$ **C**. Then, oxidative addition of Ir(III) into the *ortho* C–H bond provided Ir(V)–aryl intermediate **D**. Intermediate **D** then under reductive elimination delivered the borylated product **84** and the Ir(III)–H intermediate **E**. The regeneration of the active catalyst involved the attachment of B_2pin_2 to intermediate **E** to form complex **F**. B_2pin_2 inserted to the Ir center in **F** to yield the hexa-coordinate Ir(V) intermediate **G**. Finally, the removal of HBpin through reductive elimination resulted in the active catalyst **A**. This HBpin molecule can be inserted to the Ir center of intermediate **E**, releasing H_2 via reductive elimination to obtain the active catalyst **A** (Scheme 50).

2.4. Ru-catalyzed cross-coupling of *N*-aryl-2-aminopyridines

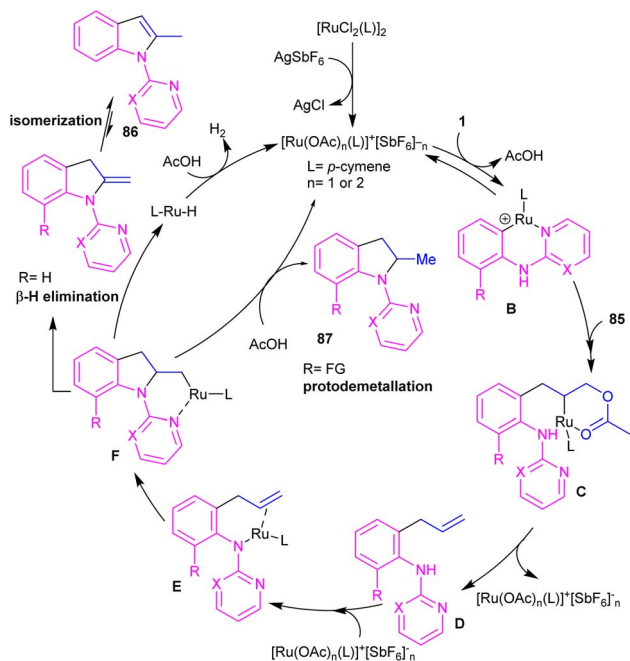
2.4.1. Annulation. A cascade C–H allylation/oxidative annulation of *N*-aryl-2-aminopyridines or *N*-aryl-2-aminopyrimidines with electron-deficient alkenes was reported by Jana and his team in 2018 (Scheme 51).⁵⁹ In the case of *N*-aryl-2-aminopyridines as a substrate, β -hydride elimination from the σ -alkyl-Ru intermediate led to 2-methylindoles, while for *N*-aryl-2-aminopyrimidine substrates, due to the suppression of β -hydride elimination by steric effect in interaction with the pyrimidine group which stabilized the alkyl-Ru species through coordination, a protodemetalation occurred *in lieu* of



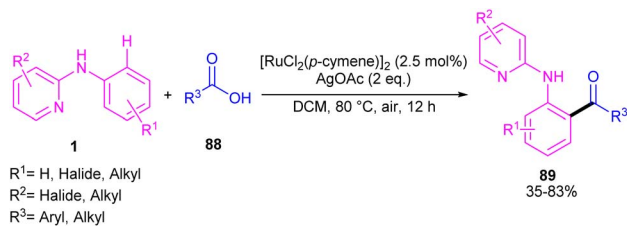


Scheme 51 Ru(II)-catalyzed C–H allylation/oxidative annulation of *N*-aryl-2-aminopyridines or *N*-aryl-2-aminopyrimidines with electron-deficient alkenes.

β -hydride elimination. The authors proposed a mechanism for the Ru(II)-catalyzed cascade reaction as shown in Scheme 52. It was proposed that *ortho* C–H activation of **1** with the active ruthenium complex generated intermediate **B**, which underwent migratory insertion of alkene to obtain an alkyl ruthenium intermediate **C**. Then, β -acetoxy elimination gave allylation intermediate **D**. Further coordination of the Ru with the nitrogen and subsequent alkene insertion to the allyl group resulted in intermediate **F**. In the case of *ortho*-unsubstituted *N*-aryl-2-aminopyrimidines, **F** underwent a rapid β -hydride elimination and double bond isomerization to yield product **86**. Whereas, for the *ortho*-substituted *N*-aryl-2-aminopyrimidines **33**, the protodemetalation in the protic solvent, like TFE,



Scheme 52 Plausible mechanism for Ru(II)-catalyzed C–H allylation/oxidative annulation of *N*-aryl-2-aminopyridines or *N*-aryl-2-aminopyrimidines with electron-deficient alkenes.

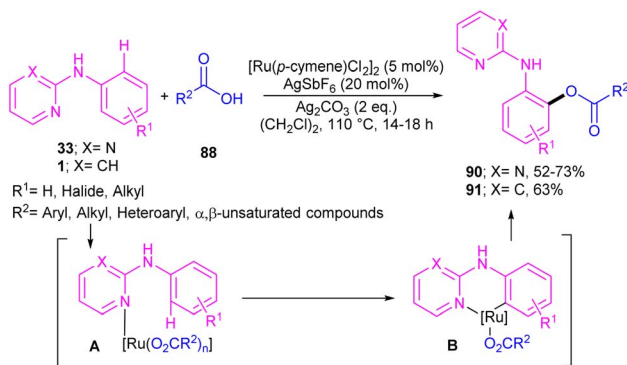


Scheme 53 Ru(II)-catalyzed C–H acylation of aniline derivatives with α -oxocarboxylic acids.

afforded product **87**. The generated ruthenium hydride species in this step was converted to the active catalyst *via* the interaction of H_2 gas with AcOH. Indole derivatives can also be achieved through ruthenium-catalyzed annulation of *N*-aryl-2-aminopyridines with α -carbonyl sulfoxonium ylides.⁶⁰ However, $[\text{IrCp}^*\text{Cl}_2]_2$ and $[\text{RhCp}^*\text{Cl}_2]_2$ resulted in very low yield of product, and $\text{Cp}^*\text{Co}(\text{CO})\text{I}_2$ did not workable.

2.4.2. Functionalization

2.4.2.1. Acylation and acetoxylation. Li and co-workers described *ortho*-acylation of *N*-(2-pyridyl)-anilines **1** with arylglyoxylic acids **88** under ruthenium catalysis (Scheme 53).⁶¹ *N*-(2-Pyridyl)-anilines bearing electron-donating and aryl and heteroaryl glyoxylic acids electron-withdrawing groups at the both pyridine and benzene ring were evaluated, in which electron-rich substrates showed better reactivity than electron-deficient ones. In the case of arylglyoxylic acids, a certain order was not realized, while heteroaryl glyoxylic acids like 2-thiophenylglyoxylic acid and 2-furanyl glyoxylic acid led to slightly lower products. Overall reaction mechanism involved pyridine-assisted direct $\text{C}(\text{sp}^2)\text{-H}$ bond activation *via* CMD pathway, acid coordination, decarboxylation, and reductive elimination. The ruthenium/silver catalysis was found to be workable for acylating *N*-aryl-2-aminopyridine or *N*-aryl-2-aminopyrimidines (Scheme 54).⁶² Carboxylic acids were selected as acylating reagents, which were coordinated with the metal center of complex **A**, followed by the reductive elimination towards the acylated product **90**, **91**.

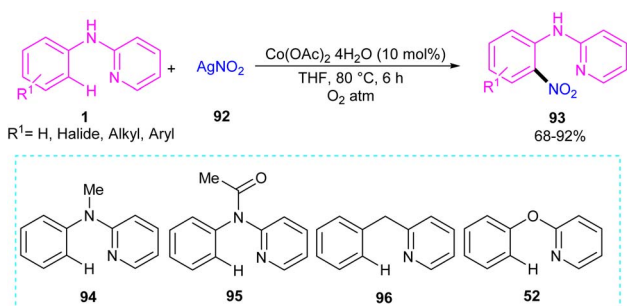


Scheme 54 Ru(II)-catalyzed C–H acylation of *N*-aryl-2-aminopyridines or *N*-aryl-2-aminopyrimidines with carboxylic acids.

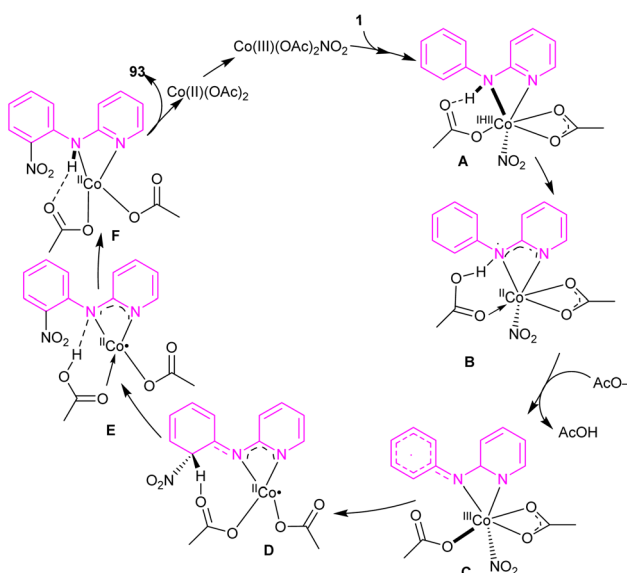


2.5. Co-catalyzed cross-coupling of *N*-aryl-2-aminopyridines

2.5.1. Nitration. An efficient nitration method for *N*-phenyl-2-aminopyridine **1** was described by Das's group in 2017 (Scheme 55).⁶³ By using an $\text{Co}(\text{OAc})_2$ catalyst, nitration of *N*-phenyl-2-aminopyridine with AgNO_3 was achieved in good yields (70–92%). *N*-Thiophene-2-aminopyridine was also nitrated under cobalt catalysis in 68% of yield. The cobalt acetate can also catalyze the methoxylation of *N*-phenyl-2-aminopyridine using methanol as both a coupling partner and solvent. Mechanistic experiments were performed, and these allowed the authors to conclude that the reaction proceeded through a radical pathway and the C–H activation was not the rate-determining step. Interestingly, none of the substrates **94**, **95**, **96**, and **52** were not compatible which proved the vital role of the NH in the coordination chemistry with the metal. The mechanism of the reaction started with the generation of reactant complex (RC) from the active catalyst $\text{Co}(\text{III})(\text{OAc})_2(\text{NO}_2)$ and *N*-aryl-2-aminopyridine. Through a PCET reaction, a proton in RC transferred to acetate, leading to the reduction of $\text{Co}(\text{III})$ reduced to $\text{Co}(\text{II})$. Due to the high energy barrier for the nitro



Scheme 55 $\text{Co}(\text{II})$ -catalyzed regioselective $\text{C}(\text{sp}^2)$ -H bond nitration of *N*-phenyl-2-aminopyridine.

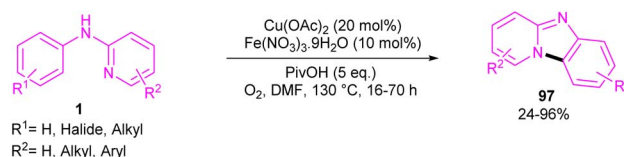


Scheme 56 Catalytic cycle for $\text{Co}(\text{II})$ -catalyzed regioselective $\text{C}(\text{sp}^2)$ -H bond nitration of *N*-phenyl-2-aminopyridine.

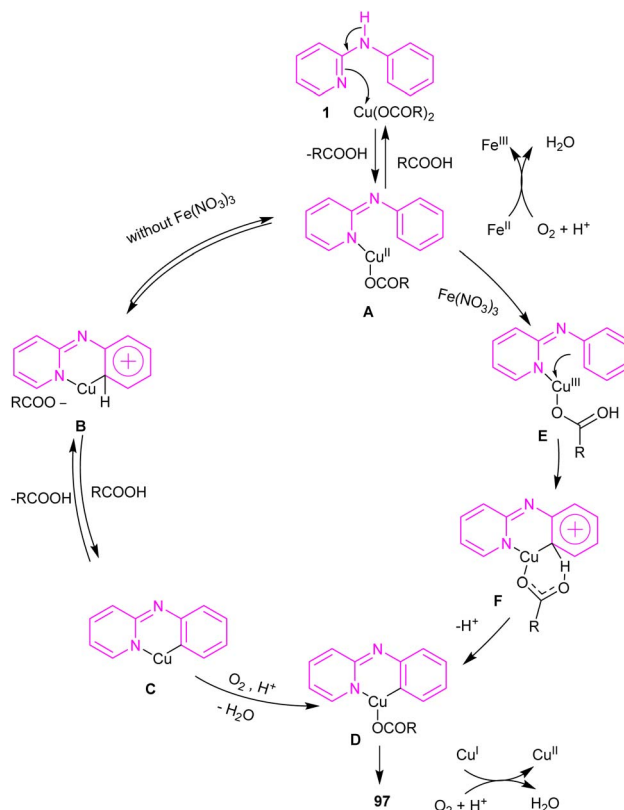
group transfer from $\text{Co}(\text{II})$ to phenyl group, acetic acid group exchanged with an acetate ion to form a $\text{Co}(\text{III})$ complex **12**. The transfer of nitro functional group from **12** gave complex **13**. In **13**, H-transfer reaction offered intermediate **14**. Further proton transfer to the imino-functional group from AcOH provided intermediate **15**. Finally, complex **15** converted to the nitrated product after the release of $\text{Co}(\text{OAc})_2$ (Scheme 56).

2.6. Cu-catalyzed cross-coupling of *N*-aryl-2-aminopyridines

2.6.1. Annulation. An intramolecular C–H amination of *N*-phenyl-2-aminopyridine derivatives was established using $\text{Cu}(\text{OAc})_2$ as a catalyst (Scheme 57).⁶⁴ The pyridinyl nitrogen was found to be both a directing group and a nucleophile. Screening of this transformation in the presence of $\text{Fe}(\text{NO}_3)_3 \cdot 9\text{H}_2\text{O}$ and without it, showed the significant role of $\text{Fe}(\text{NO}_3)_3 \cdot 9\text{H}_2\text{O}$ in increasing of the reaction efficiency. The iron(III) helped in forming the electrophilic $\text{Cu}(\text{III})$ species, leading to the

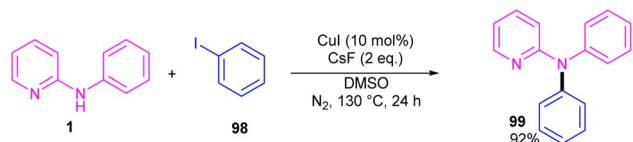


Scheme 57 $\text{Cu}(\text{II})$ -catalyzed intramolecular C–H amination of *N*-phenyl-2-aminopyridine.



Scheme 58 Proposed reaction pathways for $\text{Cu}(\text{II})$ -catalyzed intramolecular C–H amination of *N*-phenyl-2-aminopyridine.





Scheme 59 Cu(I)-catalyzed *N*-arylation of *N*-phenyl-2-aminopyridine.

subsequent S_EAr reaction. In this context, two possible pathways were proposed in the presence and absence of iron(III). In the first case, the Cu(II) complex **A** was oxidized to the more electrophilic Cu(III) intermediate **E**, followed by sequentially electrophilic substitution, and elimination of the aromatic proton to yield intermediate **D**. Reductive elimination then took place before protonation to furnish pyrido[1,2-*a*]benzimidazoles **97**. However, without Ir(III) salt, the Cu(II) complex **A** underwent an electrophilic aromatic substitution to render the Cu(II) intermediate **C**. After that, **C** was protonated before the oxidation process. The generated active intermediate **D** was then converted to product **97** *via* reductive elimination. The oxidation of Cu(I) to Cu(II) was carried out by O_2 (Scheme 58).

2.6.2. Arylation. Copper-catalyzed *N*-arylation of *N*-phenyl-2-aminopyridine **1** was reported by Ribas and Güell in 2014 (Scheme 59).⁶⁵ The C–N cross-coupling was carried out in the presence of 10 mol% of CuI and 2 equiv. of CsF in DMSO. This method has presented a ligand-free Ullmann-type C–N bond coupling. DMSO served both as a solvent and ligand, overcoming the need for any external auxiliary ligands. A wide range of amines exhibited good compatibility in this methodology.

3. Conclusions

In this review, we presented developments on *N*-aryl-2-aminopyridines reactions under transition metal catalysis systems. As shown in this context, the nitrogen atom in the pyridyl group structure can form a series of more stable complexes with metals, leading to annulation or functionalization of *N*-aryl-2-aminopyridines. Various transition metal catalysts, such as Pd, Rh, Ir, Ru, Co and Cu salts can efficiently catalyze the transformations involving *N*-aryl-2-aminopyridines. Despite the great developments, these synthetic methods still face some disadvantages, such as high temperatures, the use of external oxidants and additives for the C–H activation reactions. Hence, designing greener and milder procedures in this field is highly desirable. In particular, the functionalization of *N*-aryl-2-aminopyridines still requires a lot of work.

Considering the sustainability and effectiveness of photocatalysis and electrocatalysis systems, it is worth mentioning that the combination of these two catalytic systems with metal containing systems can constitute an efficient multiple catalytic system for transforming *N*-aryl-2-aminopyridines.

We hope that this review will provide new insights into the chemistry and transformations of *N*-aryl-2-aminopyridines to design more practical and sustainable methods in the field of *N*-heterocyclic chemistry.

Data availability

The data supporting the findings of this study are available within the article.

Conflicts of interest

There are no conflicts to declare.

Notes and references

- S. Rej, Y. Ano and N. Chatani, *Chem. Rev.*, 2020, **120**, 1788–1887.
- S. Sunny and R. Karvembu, *Adv. Synth. Catal.*, 2021, **363**, 4309–4331.
- G. Rouquet and N. Chatani, *Angew. Chem., Int. Ed.*, 2013, **52**, 11726–11743.
- J. Jeon, C. Lee, I. Park and S. Hong, *Chem. Rec.*, 2021, **21**, 3613–3627.
- O. Daugulis, J. Roane and L. D. Tran, *Acc. Chem. Res.*, 2015, **48**, 1053–1064.
- L. Merces and M. Albrecht, *Chem. Soc. Rev.*, 2010, **39**, 1903–1912.
- H. Song, E. Pietrasiak and E. Lee, *Acc. Chem. Res.*, 2022, **55**, 2213–2223.
- A. Amin, T. Qadir, P. K. Sharma, I. Jeelani and H. Abe, *Open Med. Chem. J.*, 2022, **16**, 1–27.
- A. Omar, *Al-Azhar J. Pharm. Sci.*, 2020, **62**, 39–54.
- T. Qadir, A. Amin, P. K. Sharma, I. Jeelani and H. Abe, *Open Med. Chem. J.*, 2022, **16**, 1–34.
- D. Kumar and S. Kumar Jain, *Curr. Med. Chem.*, 2016, **23**, 4338–4394.
- E. Stempel and T. Gaich, *Acc. Chem. Res.*, 2016, **49**, 2390–2402.
- S. M. Umer, M. Solangi, K. M. Khan and R. S. Z. Saleem, *Molecules*, 2022, **27**, 7586.
- C. Prandi and E. G. Occhiato, *Pest Manage. Sci.*, 2019, **75**, 2385–2402.
- K. W. Anderson, R. E. Tundel, T. Ikawa, R. A. Altman and S. L. Buchwald, *Angew. Chem., Int. Ed.*, 2006, **45**, 6523–6527.
- Q. Shen, T. Ogata and J. F. Hartwig, *J. Am. Chem. Soc.*, 2008, **130**, 6586–6596.
- S. Hostyn, G. Van Baelen, G. L. Lemiere and B. U. Maes, *Adv. Synth. Catal.*, 2008, **350**, 2653–2660.
- G.-D. Tang, C.-L. Pan and X. Li, *Org. Chem. Front.*, 2016, **3**, 87–90.
- A. Khadra, S. Mayer and M. G. Organ, *Chem.–Eur. J.*, 2017, **23**, 3206–3212.
- T. T. Deng, J. Huang, G. Lian, W. W. Sun and B. Wu, *Asian J. Org. Chem.*, 2021, **10**, 2880–2882.
- F. Tjosaas and A. Fiksdahl, *J. Organomet. Chem.*, 2007, **692**, 5429–5439.
- B. Ramesh and M. Jeganmohan, *Org. Lett.*, 2017, **19**, 6000–6003.
- Y. Luo, L. Guo, X. Yu, H. Ding, H. Wang and Y. Wu, *Eur. J. Org. Chem.*, 2019, 3203–3207.



Review

- 24 J. Chen, Q. Pang, Y. Sun and X. Li, *J. Org. Chem.*, 2011, **76**, 3523–3526.
- 25 J. Chen, K. Natte, A. Spannenberg, H. Neumann, M. Beller and X. F. Wu, *Chem.–Eur. J.*, 2014, **20**, 14189–14193.
- 26 Q. Li, M. Zhu, X. Yan, Y. Xia and X. Zhou, *J. Organomet. Chem.*, 2021, **948**, 121930.
- 27 W. Guo, W. Hu, X. Zhang, J. Huang, H. Wang, M. Xia and L. Tao, *Asian J. Org. Chem.*, 2024, **13**, e202300651.
- 28 P. V. Reddy, M. Annapurna, P. Srinivas, P. R. Likhari and M. L. Kantam, *New J. Chem.*, 2015, **39**, 3399–3404.
- 29 J. H. Chu, P. S. Lin, Y. M. Lee, W. T. Shen and M. J. Wu, *Chem.–Eur. J.*, 2011, **17**, 13613–13620.
- 30 D. Liang, Y. He and Q. Zhu, *Org. Lett.*, 2014, **16**, 2748–2751.
- 31 J. Chen, K. Natte and X.-F. Wu, *J. Organomet. Chem.*, 2016, **803**, 9–12.
- 32 U. Sharma, R. Kancherla, T. Naveen, S. Agasti and D. Maiti, *Angew. Chem., Int. Ed.*, 2014, **53**, 11895–11899.
- 33 L. Jie, L. Wang, D. Xiong, Z. Yang, D. Zhao and X. Cui, *J. Org. Chem.*, 2018, **83**, 10974–10984.
- 34 X. Ding, L. Zhang, Y. Mao, B. Rong, N. Zhu, J. Duan and K. Guo, *Synlett*, 2020, **31**, 280–284.
- 35 S. H. Kim, S. H. Park and S. Chang, *Tetrahedron*, 2012, **68**, 5162–5166.
- 36 J. Xu, X. Li, S. Wang, C. Kang, G. Jiang and F. Ji, *J. Org. Chem.*, 2023, **88**, 6168–6175.
- 37 K. Yang, Q. Li, Z. Li and X. Sun, *Chem. Commun.*, 2023, **59**, 5343–5364.
- 38 J. Chen, G. Song, C.-L. Pan and X. Li, *Org. Lett.*, 2010, **12**, 5426–5429.
- 39 Z.-J. Wu, K. L. Huang and Z.-Z. Huang, *Org. Biomol. Chem.*, 2017, **15**, 4978–4983.
- 40 X. Hu, X. Chen, Y. Zhu, Y. Deng, H. Zeng, H. Jiang and W. Zeng, *Org. Lett.*, 2017, **19**, 3474–3477.
- 41 X. Yan, R. Ye, H. Sun, J. Zhong, H. Xiang and X. Zhou, *Org. Lett.*, 2019, **21**, 7455–7459.
- 42 Z. Shen, C. Pi, X. Cui and Y. Wu, *Chin. Chem. Lett.*, 2019, **30**, 1374–1378.
- 43 S. He, X. Yan, Y. Lei, H. Xiang and X. Zhou, *Chem. Commun.*, 2020, **56**, 2284–2287.
- 44 Y. Wang, D. Jia, J. Zeng, Y. Liu, X. Bu and X. Yang, *Org. Lett.*, 2021, **23**, 7740–7745.
- 45 S. K. Keshri, S. Madhavan and M. Kapur, *Org. Lett.*, 2022, **24**, 9043–9048.
- 46 P. Biswal, T. Nanda, N. Prusty, S. R. Mohanty and P. C. Ravikumar, *J. Org. Chem.*, 2023, **88**, 7988–7997.
- 47 N. K. Mishra, M. Choi, H. Jo, Y. Oh, S. Sharma, S. H. Han, T. Jeong, S. Han, S.-Y. Lee and I. S. Kim, *Chem. Commun.*, 2015, **51**, 17229–17232.
- 48 S. Yang, B. Feng and Y. Yang, *J. Org. Chem.*, 2017, **82**, 12430–12438.
- 49 Q. Liu, Z. Ma, J. Zhang and X.-Q. Li, *Org. Biomol. Chem.*, 2023, **21**, 8320–8328.
- 50 J. Yang, W. Shi, W. Chen, H. Gao, Z. Zhou and W. Yi, *J. Org. Chem.*, 2021, **86**, 9711–9722.
- 51 Z. J. Wu, F. Su, W. Lin, J. Song, T. B. Wen, H. J. Zhang and H. C. Xu, *Angew. Chem.*, 2019, **131**, 16926–16930.
- 52 S. Bai, X. Chen, X. Hu, Y. Deng, H. Jiang and W. Zeng, *Org. Biomol. Chem.*, 2017, **15**, 3638–3647.
- 53 U. Karmakar, D. Das and R. Samanta, *Eur. J. Org. Chem.*, 2017, 2780–2788.
- 54 J. Xia, X. Yang, Y. Li and X. Li, *Org. Lett.*, 2017, **19**, 3243–3246.
- 55 X. Zhou, J. Xia, G. Zheng, L. Kong and X. Li, *Angew. Chem., Int. Ed.*, 2018, **57**, 6681–6685.
- 56 X.-F. Cui, X. Qiao, H.-S. Wang and G.-S. Huang, *J. Org. Chem.*, 2020, **85**, 13517–13528.
- 57 G.-D. Tang, C.-L. Pan and F. Xie, *Org. Biomol. Chem.*, 2016, **14**, 2898–2904.
- 58 M. M. Mahamudul Hassan, B. Mondal, S. Singh, C. Haldar, J. Chaturvedi, R. Bisht, R. B. Sunoj and B. Chattopadhyay, *J. Org. Chem.*, 2022, **87**, 4360–4375.
- 59 M. K. Manna, G. Bairy and R. Jana, *J. Org. Chem.*, 2018, **83**, 8390–8400.
- 60 X.-F. Cui, Z.-H. Ban, W.-F. Tian, F.-P. Hu, X.-Q. Zhou, H.-J. Ma, Z.-Z. Zhan and G.-S. Huang, *Org. Biomol. Chem.*, 2019, **17**, 240–243.
- 61 Q. Liu, J.-Y. Yong, J. Zhang, T. Ban and X.-Q. Li, *Org. Biomol. Chem.*, 2022, **20**, 6890–6896.
- 62 T. Sarkar, S. Pradhan and T. Punniyamurthy, *J. Org. Chem.*, 2018, **83**, 6444–6453.
- 63 D. Nageswar Rao, S. Rasheed, G. Raina, Q. N. Ahmed, C. K. Jaladanki, P. V. Bharatam and P. Das, *J. Org. Chem.*, 2017, **82**, 7234–7244.
- 64 H. Wang, Y. Wang, C. Peng, J. Zhang and Q. Zhu, *J. Am. Chem. Soc.*, 2010, **132**, 13217–13219.
- 65 I. Güell and X. Ribas, *Eur. J. Org. Chem.*, 2014, 3188–3195.

